

MODELING AND ANALYSIS OF A BLAST RESISTANT UNDERGROUND BUNKER WITH FINITE ELEMENT METHOD

Project submitted by

PRIYADARSHI MUKHOPADHYAY

Roll Number: 21CE8022

Under the guidance of

Dr. Pronab Roy

Department of Civil Engineering

National Institute of Technology, Durgapur -713209



**NATIONAL INSTITUTE OF TECHNOLOGY
DURGAPUR**

NATIONAL INSTITUTE OF TECHNOLOGY
DURGAPUR
DEPARTMENT OF CIVIL ENGINEERING



CERTIFICATE

This is to certify that the thesis entitled *Modeling and Analysis of a Blast-Resistant Underground Bunker with Finite Element Method* submitted by Priyadarshi Mukhopadhyay, Roll Number 21CE8022, in partial fulfillment of the requirements for the Bachelor of Technology degree in Civil Engineering is a bona fide record for the work carried out by him at the Department of Civil Engineering, National Institute of Technology, Durgapur under my guidance and supervision.

Dr. P. Topadar,
Head Of The Department,
Civil Engineering,
NIT Durgapur

Dr. Pronab Roy,
Professor
Department of Civil Engineering,
NIT Durgapur

DECLARATION

I hereby declare that the thesis entitled *Modeling and Analysis of a Blast-Resistant Underground Bunker with Finite Element Method* submitted in the Department of Civil Engineering, National Institute of Technology, Durgapur in partial fulfillment of the requirement for the award of the B.Tech. degree in Civil Engineering is an authentic work carried out by me under the supervision of Dr. Pronab Roy, Professor, Civil Engineering Department, NIT, Durgapur. The matters presented in this thesis represent my ideas, in my own words, and where other ideas or words have been included, citations and references of the original work have been provided. I also declare that I have adhered to all principles of academic honesty and integrity and have not misrepresented or falsified any idea, data, fact, source in my submission. I understand that any violation of the award will cause for disciplinary action by the Institute and can evoke penal action from the sources which have thus not been properly cited or from whom permission has not been taken.

PRIYADARSHI MUKHOPADHYAY

21CE8022

ACKNOWLEDGEMENT

I thank Dr. Pronab Roy for guiding me through this project - *Modeling and Analysis of a Blast-Resistant Underground Bunker with Finite Element Method* -with the conception, the structure, the proceedings and the flow of the project.

I thank Dr. P. Topadar and Dr. A. K. Datta for teaching me Finite element method, which has been incorporated here.

Above all, I thank my mother who always tried to keep me in the sane side of things.

I thank my father for bearing with me with a smile on his face.

PRIYADARSHI MUKHOPADHYAY

21CE8022

ABSTRACT

A bunker is an underground reinforced concrete structure intended to safeguard human lives and critical assets during hostile events such as military or terrorist attacks. With the increasing frequency of such incidents globally- which includes the wars in the present times, the construction of bunkers is gaining renewed importance. Thus it is important with changing times to accommodate to the global importance on construction of bunkers alongside other major national endeavors. In this study we are going to model and study the blast-resistant bunker, a shelter that stands against blast load when residential buildings collapse. This study presents the modeling and analysis of a blast-resistant underground bunker using the Finite Element Method. Simulations were performed on finite element softwares for different charge standoff distances and soil types (clay and sand). The results show that while increasing the charge weight and decreasing the standoff distance increase deformation, the choice of soil has a significantly greater effect. Clay soil demonstrated better damping of blast-induced vibrations, leading to lower deformation values. The study concludes that soil selection is a crucial parameter in bunker design, influencing the overall safety and resilience of underground protective structures.

CONTENTS

1. Introduction	5
2. Background	17
3. Methodology	22
3.1 Finite Element Method	24
3.2 Model Specification	28
3.3 Geometry of the Model	29
3.4 Solid Properties	39
3.5 Soil Properties	44
3.6 Meshing	47
3.7 Blast Load	50
4. Results And Discussion	54
5. Conclusions	61
6. Citations	62
7. Bibliography	63

LIST OF FIGURES

Fig 1.1 (author)	6
Fig 1.2-1.6 (wikipedia)	6 to 15
Fig 2.1 (author)	17
Fig 2.2-2.3 (5)	20
Fig 3.1 – 3.23 (author)	23 to 52
Fig 4.1-4.6 (author)	54 to 59

LIST OF TABLES

Table 2.1	22
Table 3.1	30
Table 3.2	43
Table 3.3	44
Table 3.4	45
Table 3.5	47
Table 3.6	50
Table 3.7	50
Table 3.8	54
Table 4.1	57
Table 4.2	57
Table 4.3	57

1. INTRODUCTION

There has always been a need for something more than ordinary shelter. Regular homes can't stand against certain threats—bombs, raids, shockwaves. So people built something separate. Hidden. Strong. A shelter that wouldn't look like one. That's how bunkers came to be. During times of war, their construction rose sharply. Especially underground. A separate place for safety. A separate space for survival.

Bunkers are fortified shelters, primarily underground, designed to protect people and vital materials from aerial attacks, artillery, or other threats. They became prominent during World War I and even more so in World War II, evolving into strategic strongholds for both civilian and military use. In Britain, structures like the Anderson shelter—made of corrugated steel and installed in gardens—offered families refuge during air raids. Underground stations and purpose-built tunnels, such as the London deep-level shelters, provided mass protection, housing thousands during the Blitz. In Germany, massive concrete bunkers, or Hochbunkers, were constructed to shield urban populations. These shelters did more than protect lives—they represented a mindset shaped by conflict, a clear emphasis on civil defense, on survival, on preparedness for the worst.

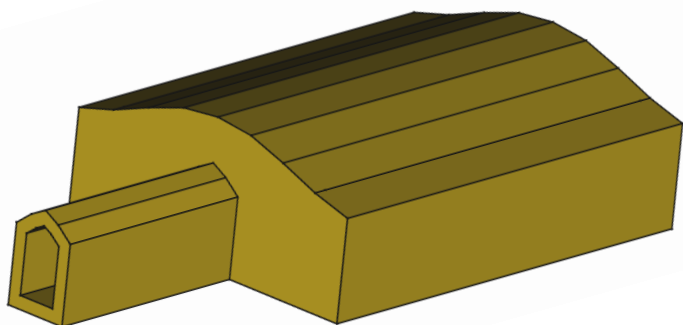


Fig 1.1 The structure of a typical under-ground bunker. This kind of shelter had been used for safety against air-raids. They were popular during World War 2.

In the beginning, there were no definite structures called bunkers to protect soldiers on the battlefield. In the First World War, English soldiers dug into the earth and made what they called dugouts—crude underground shelters. These were not proper constructions. They lacked building materials, and living conditions were harsh, damp, and cold. The Germans used the term “bunker,” but their shelters were also just deep trenches—underground spaces at best.

By the Second World War, this changed. Permanent structures began to appear underground—made of concrete, steel, and brick. Both Germany and Britain started building true bunkers.

Strong, sealed, and made to last. In Britain, Anderson shelters were installed in backyards. In Germany, massive Hochbunkers rose in cities. As the war intensified, Japan began building bunkers across urban areas to protect civilians from American air raids. That was when bunkers came into wide use.

During the Winter War, Finland built civilian bunkers to guard against the threat of Russian air attacks. Bunkers, once a desperate invention, had become part of how people prepared for the worst—an underground answer to danger from above.



Fig 1.2 The entrance of an underground bunker in Kleines Berlin, The inside of one underground tunnel. They were built by Germany in 1943 after annexing the Adriatic coast in Italy. [\(1\)](#)

Bunkers can come in various types, depending on the kind of emergency they try to meet and the people they want to shelter. Also, the place where they are built, the circumstances and time and material constraints are of paramount importance. They typically come in the following types:

Trench Bunkers

Trenches are the earliest type of bunkers. They are dug quickly when there is no time to build permanent shelters. A bit of concrete is sometimes used, but mostly it is just earth. They protect soldiers from bullets and air attacks. They are temporary, dirty, and harsh. They are typically built in battle grounds and fields of attacks.

Artillery Bunkers

Artillery bunkers house large guns, ammunition, and supplies. Ammunitions are always something that enemy would like to destroy instead of engaging in a direct conflict, as evident during these times of cold wars. These are found near coastlines or in fixed military zones. They are strong and hard to destroy. They exist to keep the weapons firing and the enemy away.

Industrial Bunkers

Industrial bunkers are built near mines, refineries, or storage areas. They protect raw materials, machines, and sometimes workers. In modern warfare, resources are targets. Often cross nation conflicts arise due to the presence of rich materials like rare earth (as evident in the war between Russia and Ukraine that began in 2022). Thus, it is necessary to store these rich materials which are primary enemy targets as revenue comes from them. These bunkers are meant to keep them safe.

Personal Bunkers

Personal bunkers are built by individuals who want to survive on their own. They are usually underground and stocked with food, water, and medicine. These bunkers are small, isolated, and meant for long periods without contact. During times of conflict, people have shown to enter into a psychological survival mechanism. Personal Bunkers have been seen especially during those times, where people build a defensive shelter in their backyard for protection.



Fig 1.3 The US Army Fallout Shelter sign board (1961), The Sonnenberg Tunnel in Switzerland – the largest nuclear bunker (fallout shelter) designed to protect 20000 civilians. [\(1\)](#)

Munitions Storage Bunkers

These bunkers store explosives like TNT, Uranium and other dangerous materials. They are dome-shaped and often dug into hillsides. The walls are thick enough to contain a blast if something goes wrong inside as well as protect those explosives from external triggers.

Airstrike Bunkers

Airstrike bunkers protect civilians during aerial bombings. They were used heavily during the Second World War, especially in cities like London and Japan. People would hide in subway stations, gardens, or underground shelters while the city above were reduced down to rubbles.

Fallout Shelters

Fallout shelters are designed for nuclear attacks. They are deep underground, with walls thick

enough to block radiation. These shelters are reserved for key figures—politicians, scientists, and military leaders. They are meant to keep power alive after everything else is gone. Even large scale civilian bunkers are built as fallout shelters to protect them against nuclear threats. One may remember a horrible massacre of civilization that happened in Hiroshima and Nagasaki after these two cities were reduced to nothing by US nuclear bombs. It is important to protect people against such life denying forces.

The most common kind of attack is the air raid. It doesn't kill in one blow. It works over time—cheap, strategic, and organized. Bombs drop in intervals, one after another, in rhythm. The goal is to weaken, not wipe out in a single strike. Cities suffer damage not only at the point of impact but also in the surrounding structures. Buildings nearby collapse from shockwaves, heat, and pressure. Walls crack, windows shatter, roofs give way—without a direct hit.

This kind of destruction has worsened as bombing technology evolved. The damage spreads wider. The targets shift from specific military points to general city zones. The intention is to cripple—not just physically, but economically and mentally. It's fast. It's systematic. It's hard to blame. During the wars in Vietnam and Afghanistan, this pattern became common. Randomized raids were carried out to avoid the appearance of war crimes while still creating large-scale collapse. Entire neighborhoods fell under pressure that never touched them directly.



Fig 1.4 Aftermath of an air raid in Vietnam- residential buildings collapsed, A B-2 Spirit US AirCraft launching Mark 82 (500kg Charge weight) bombs in an indiscriminate manner. Mark-80 series were common General purpose arsenals that were made of TNT in Aluminium boxes. [\(1\)](#)

As the world moved beyond the Cold War, a new kind of threat emerged—terror. Societal residencies became targets. Localities. High-rise buildings. Crowded spaces. The aim changed. It wasn't just disruption; it was spectacle. It was fear. Attacks were launched in congested zones where even an imprecise strike would bring everything nearby to the ground. Markets. Apartments. Offices. You see, the most unprecedented phenomenon was this: even when the target wasn't accurate, the damage happened anyway. Places that were never under direct attack collapsed. Neighborhoods next to the blast site shattered—glass, concrete, metal all

giving way to a pressure they weren't built to handle. This wasn't tactical anymore. It was ambient destruction. The shockwaves spread farther than expected. Entire blocks were lost without a direct hit. That changed how cities had to think about protection. It wasn't about guarding the center anymore. It was about defending everything around it too. That's when the need for deeper, wider, civilian-focused bunkers began to feel real.



Fig 1.5 The Oklahoma City bombing- Alfred-Murray Building, Aerial View of Oklahoma City. We see wide scale structural damage not only at the site of attack but also in the surrounding neighborhood. This is a typical phenomenon of blast-which is the result of explosive attacks that occur in a short section of time. (1)

In the century of wars that preceded this time where war has only intensified, it has been observed that a Peripheral collateral damage of structural sites happen alongside the damage that the site under attack experiences. Localized terror attacks cause wide scale damage even when they run short of ammunitions. Refer to fig 1.5 to see how such massive such localised attacks are.

Peripheral collateral damage is the destruction that occurs not at the direct site of an attack, but in the surrounding areas—sometimes blocks away. It's the apartment next to the targeted building that collapses. It's the office across the street that shatters. It's the structure that wasn't meant to break, but did.

This happens because of the **blast phenomenon**.

When a high explosive detonates, it creates an extremely rapid release of energy—with microseconds. This release compresses the air around it, forming a **blast wave**, also called a **shock front**. This wave travels faster than sound, pushing outward with intense pressure. At the point of detonation, the damage is absolute. But the wave keeps moving—into buildings, streets, and walls nearby.

Even if a structure isn't hit by the explosion itself, it absorbs this pressure. Windows implode. Doors are ripped off. Walls crack. In reinforced buildings, the internal stress may remain invisible at first—until over time, they fail.

There are three key effects in a blast:

1. **Overpressure:** A sudden rise in atmospheric pressure that crushes materials.
2. **Dynamic pressure:** The wind-like push that follows the blast wave.
3. **Reflected waves:** When the blast bounces off surfaces, amplifying its force.

In congested urban spaces, these effects multiply. The blast bounces between buildings. Corners amplify force. Pressure gets trapped. That's why even distant or "safe" structures collapse. It's not randomness. It's physics, misunderstood or ignored.

In military terms, the zone affected by these forces is called the secondary damage radius. In cities, it's chaos.

The deeper tragedy is this: even when an attack misses its mark, the surroundings don't survive. That's the reality of modern bombing. That's peripheral collateral damage—silent, wide, and inevitable.

In the study of explosions and their effects on surroundings, two names stand out prominently—Friedrich Friedlander and G.I. Taylor—both of whom contributed significantly to our understanding of how blast waves behave in air and how they inflict damage not just at the point of explosion but also in surrounding regions. These two scientists approached the problem from different directions—one from the temporal pressure response at a point, and the other from the spatial propagation of the blast front—and together, their insights laid the groundwork for modern blast theory used in military defense, structural engineering, and safety design. The story begins in the early to mid-20th century when scientists were first trying to understand the devastating nature of explosions, particularly after witnessing large-scale wartime detonations and eventually, nuclear blasts. Friedrich Friedlander, a German physicist, was one of the first to attempt modeling the pressure-time profile of a blast wave as experienced at a stationary point some distance away from the explosion. He proposed what is now called the Friedlander waveform, a characteristic curve showing a sharp rise in pressure as the shock wave arrives (the "shock front"), followed by a steady exponential decay and sometimes even a negative pressure phase (a vacuum or suction effect), which has massive implications for structural failure. This waveform helped engineers and defense scientists predict how long a structure or a person would be subjected to high pressure and how resilient a material needed to be over that duration. While Friedlander focused on what happens at a fixed point in space, G.I. Taylor, a British physicist, tackled a different but related problem: how does a blast wave expand outward from the source of the explosion? Taylor's work came to public attention when, during the Cold War, he famously estimated the energy yield of atomic bomb tests from photographs published in Life magazine. Using dimensional analysis, Taylor derived the relationship between the radius of the shockwave and the time elapsed since the detonation, producing what is now known as the Sedov–Taylor blast wave solution. This equation provided a way to estimate the energy of a blast (E) using observable

quantities like time and radius: , where is the radius of the blast wave, is time, and is the air density. While Friedlander's waveform was based on experimental observation of pressure data, Taylor's formulation was largely theoretical, backed by strong empirical confirmation. Together, these works describe the blast wave comprehensively: Friedlander's profile tells us how intense and how long the pressure from a blast will act at a single point, while Taylor's solution describes how far and how fast that blast front travels through space. Neither scientist "completed" the other's work, but their studies are inherently linked because any real-world modeling of explosions and structural response must combine both the spatial and temporal aspects of blast behavior. Taylor's equations provide the boundary conditions and dynamic input for Friedlander's pressure-time response to be meaningful in applied scenarios. Over time, especially during the post-WWII and Cold War periods, both models were refined and incorporated into military manuals, civil defense planning, and engineering design codes. The "blast wave" that we speak of today in simulations, building codes, or even in the design of bunkers, protective barriers, and urban shelters is essentially a fusion of these two pioneering efforts. So, while Friedlander was the first to characterize how a blast affects a stationary observer, Taylor was the one who predicted how that blast expands, and together, they helped the world not only understand the terrifying power of explosions but also develop strategies and structures to survive them.

The blast phenomenon—especially the way a shockwave causes peripheral damage—was first studied seriously during and after World War II, particularly after the bombings of Hiroshima and Nagasaki in 1945. The devastation there showed that destruction wasn't just at the center of impact. Buildings miles away were damaged. People who weren't in the blast zone still died from pressure and heat. This raised urgent scientific interest.

One of the earliest and most significant mathematical explanations of the blast wave came from G.I. Taylor, a British physicist.

Who was G.I. Taylor?

Sir Geoffrey Ingram Taylor (1886–1975) was a British physicist and mathematician. During World War II, he worked on problems related to fluid dynamics and shockwaves—essential to understanding explosions. He was also a member of the Manhattan Project, sent as a British delegation. And he was the first to estimate energy release due to the explosion of a nuclear fission bomb

What did he do?

In 1950, Taylor published a paper analyzing the blast wave from a nuclear fission, even though the actual data was classified. He used dimensional analysis—a mathematical method that relates physical quantities like time, distance, pressure, and energy—to derive an approximate formula for how a blast wave expands over time. We get our modern idea of blast wave from it. It uses multiple coordinates, hence large scale matrices.

He used the publicised or already released photographs from nuclear test data (like those from Operation Crossroads during his term as a member of the Manhattan), he measured the radius of the fireball at different times, and he worked in backpropagation to estimate the energy

released. His calculations were almost correct and essentially revealed the explosive yield of an atomic bomb—without access to any classified data.

The Taylor Blast Wave Equation

His work gave birth to the Sedov–Taylor solution, a fundamental model in shockwave physics. It describes how the radius of a blast wave increases over time. The solution shows:

$$R(t) \propto \left(\frac{Et^2}{\rho}\right)^{1/5} \quad \dots (1.1)$$

Where:

- R=radius of the blast at time
- E=energy of the explosion
- ρ = density of the surrounding air

This equation showed that even at a distance, the energy of the blast still had devastating force.

Why it matters:

Taylor's work helped scientists and military engineers understand that damage isn't limited to ground zero. The wave spreads. It reflects. It multiplies in urban environments. And the destruction continues beyond the direct line of attack. That's how the world began to see the peripheral collateral damage not as accident—but as a calculable, predictable result of blast physics.

So basically, the Friedlander equation is just a way to show what happens to the air right after an explosion hits. Not the moment it hits, but what happens at that spot in the seconds after. It shows how the pressure spikes and then drops—fast. It's like a sudden punch and then this fast, dying breath. The equation looks like this:

$$P(t) = P_s \left(1 - \frac{t}{t_d}\right) e^{-bt/t_d} \quad \dots (1.2)$$

where P is the pressure at time t , P_s is the peak pressure, t_d is the duration of the main pressure wave, and b is some decay factor people adjust based on how clean or chaotic the explosion is. It basically tells you: here's the peak, and then here's how fast it fades.

Now this doesn't exist on its own. Taylor—G.I. Taylor—he came way before Friedlander in this line. He worked out how fast a shockwave from a blast expands outward. Like how the radius of that blast grows over time. His thing was about the size and timing of the explosion reaching a point. The math is:

...(1.3)

$$R(t) = \beta \left(\frac{Et^2}{\rho_0} \right)^{1/5}$$

Friedlander made a major contribution to our understanding of how a blast wave behaves after an explosion. He studied the pressure-time history of the wave, and what he found was simple but crucial: the pressure doesn't just rise and fall evenly. Instead, it rises almost instantly to a sharp peak—the moment of the blast—then gradually falls off. But what's more interesting is that it doesn't stop at zero. The pressure dips below atmospheric, creating a vacuum-like suction. This negative phase is just as important as the positive one, because it pulls things inward right after the initial outward push.

Friedlander turned this observation into a mathematical model. His equation gave shape to the pressure-time curve of a typical blast wave in free air: sudden rise, a sharp peak, a steady decay, and then the negative phase. Engineers and defense scientists began using this model to test materials, design bunkers, and simulate real-world explosions in lab conditions. His work became a base template for all later blast research. While others like Taylor focused on shock front propagation and scaling laws, Friedlander zoomed into what the wave *does* after it hits. His equation doesn't try to explain the whole blast—it explains the signature, the pattern it leaves behind in the air. That signature became essential for understanding structural damage, injury patterns, and how to shield against blasts in a practical way.

Taylor's work came from a different angle. He wasn't trying to map the wave's pressure profile over time like Friedlander. Instead, he was focused on how a blast wave *spreads* through the air after a massive explosion, like an atomic bomb. What he did was take a physical event—the detonation—and use mathematics to predict how the shockwave would behave in open space. His most famous insight was scaling: that you could relate the size and speed of the blast wave to the energy of the explosion and the time since it occurred. He used dimensional analysis to get there, which sounds dry, but it wasn't. It let him figure out how fast the wavefront would move without even knowing the bomb's exact details.

During World War II, he applied this thinking to the first atomic tests. The Americans never told him how much energy the bomb released, but just from looking at photos of the blast, he back-calculated the yield of the explosion. And he was accurate. That's how powerful his equations were. His work turned the blast into a predictable, scalable event—something that could be measured and reproduced on paper before it happened in the real world. Taylor's contribution gave governments, engineers, and physicists a tool to estimate damage zones, predict structural failure, and design tests. If Friedlander gave the shape of the wave, Taylor gave it direction, speed, and reach. The two together form the foundation of modern blast physics.

Friedlander tells you what happens after the wave reaches you. Taylor tells you when it'll reach you and how big it'll be when it does. Taylor's work came during World War II. He even famously back-calculated the energy of the Hiroshima bomb from photographs, which is wild.

Together, their work became the backbone of how we understand blast waves. One says how the wave moves, the other says how it hits. It's clinical, cold math—but it maps very real destruction. It shows why damage happens far from the center. Why buildings fall even when they weren't hit directly. This isn't theoretical. It's been used in wars, in simulations, in civil defense, and it's still the logic behind bunker design.

When you talk about peripheral destruction—how places that weren't even directly hit fall apart—you're not being poetic. That's real. That's the math. It's right there in Taylor's and Friedlander's work. Taylor shows that the shockwave doesn't stop at the blast site; it keeps spreading, swelling outward like a ripple, except it's not water—it's compressed air moving faster than sound. It hits everything in its path, not all at once, but in a timed, terrifying sequence. Then Friedlander steps in and shows what that wave does to a structure once it reaches it. It doesn't just tap a wall. It slams into it, then pulls back violently as the pressure drops below normal. That's the double-hit. That's what causes buildings to crack, windows to burst, steel to twist, even if they're a few blocks away. Not under the bomb. Just near enough.

And it's always worse in tight spaces—urban setups, crowded neighborhoods, boxed-in zones where the wave bounces around, reflects off buildings, corners, tunnels. It multiplies itself. The destruction starts to behave like it has a mind. It's not even predictable after a point. That's why you see buildings collapsing in patterns no one expected. That's why, even when the military thinks it has hit a target clean, civilian neighborhoods go down with it. The pressure doesn't care about politics.

Taylor and Friedlander didn't invent war. They just made it measurable. Their work became the invisible blueprint for modern air raid analysis, for bunker design, for understanding how damage extends far beyond the so-called "impact zone." So no, these places didn't just fall by accident.

The results of Friedlander and Taylor fundamentally changed how engineers and defense strategists thought about protective structures. Before their work, bunkers and shelters were often constructed with a focus on brute strength—thick concrete walls above ground, often visible, designed to resist direct hits or shrapnel. But as warfare became more sophisticated and aerial bombing more precise and frequent, it became increasingly clear that visibility and exposure were major liabilities, and sheer thickness wasn't always enough.

Friedlander, through his study of pressure-time histories of blast waves, showed that the force of an explosion is not a simple, instantaneous spike. It is a wave that evolves with time—a rapid positive overpressure followed by a negative phase. His mathematical equation helped quantify this, allowing designers to predict how the wave would impact a structure over time. Taylor, on the other hand, provided a self-similar solution to how blast waves propagate in air. His work, based on dimensional analysis and experimental data, made it possible to estimate peak pressures and arrival times of the wave based on the size of the explosion and the distance from it.

Together, these contributions provided the tools to simulate and understand the behavior of explosions more accurately. What emerged from this was the realization that soil—when properly used—acts as a powerful dampener. When a structure is buried, the surrounding earth absorbs a significant part of the blast energy. Instead of facing the full brunt of a wave on an exposed surface, the energy disperses through the soil, reducing the peak pressure and stretching out the load over time. This insight made the case for underground construction not just as a defensive tactic, but as a scientifically validated necessity.

Camouflage was another critical advantage. Above-ground bunkers could be spotted and targeted from the air, making them vulnerable in wars increasingly dominated by airpower and guided munitions. Underground bunkers, by contrast, were far harder to locate and offered passive concealment. The dual benefit of structural protection through damping and reduced detectability made underground bunkers the default choice in modern defense planning.

Thus, what we now see as standard bunker design—subterranean, embedded in natural terrain, low-profile—is a direct outcome of the theoretical and experimental findings of Friedlander and Taylor. Their science changed how we understood explosions, and that understanding, in turn, reshaped how we protect against them.

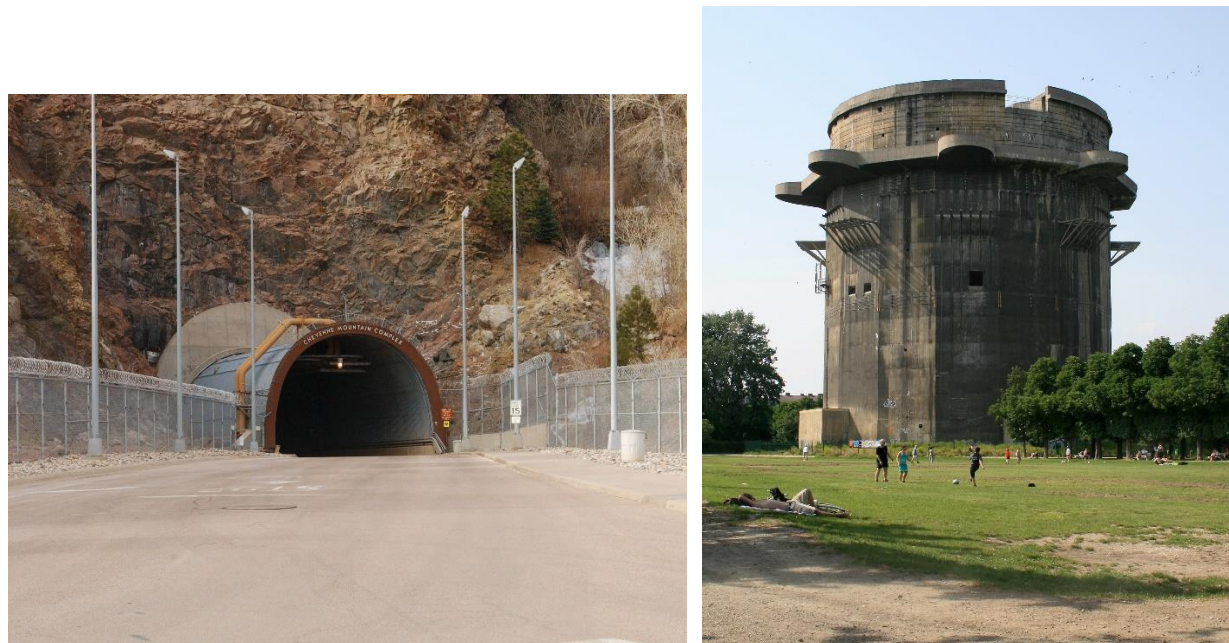


Fig 1.6 The Comparison between a modern and an old bunker- as a result of theoretical understanding of the blast phenomenon. One is underground and one is overground-erected as a tower. The north entrance to the Cheyenne Mountain Complex in Colorado, The Flakturm at the Augarten in Vienna. (1)

Bunkers are made to take the hit and unlike regular buildings, which start collapsing at something like 200 kPa overpressure (which is the typical overpressure generated by any general purpose air strike arsenal). Bunkers go past 1,000 kPa and still hold. Especially the underground ones—once you start going deep into the soil, the stress that actually reaches the bunker drops to almost nothing compared to what's happening above. It's the soil that causes just damping. Soil eats up the blast. So unless it's a direct hit with a bunker buster, nothing

much happens. That's the whole point—make a structure that just doesn't care about compression. The standard design? An RCC arched vault bunker, or sometimes buried steel versions. If one doesn't have one of those ready, people end up turning sewage pipes and metro tunnels into quick shelters (as seen in London during Blitz). Expedient shelters, they call them—half-improvised, not always safe. Purpose-built ones usually go with arched vaults buried under layers of earth. A trench is dug into a hard earth surface which is below the level of ordinary human habitation, a wooden arch is thrown and it is covered with a cloth or plastic bag, and 1-2m damped soil is dumped. It is recommended that a 2m arch length has to be provided. ⁽¹⁾ The whole idea is that when there's a ground shock—a really big one—the structure shouldn't shake itself apart. Some shocks can shift the walls of a poorly designed shelter by centimeters in milliseconds. But if you're underground, the movement drops sharply—stress is generated like 0.015 mm.

Modern bunkers have become practical, not just for the military but for civilians too. In countries like Israel, more of these structures are being built into homes and public buildings. Shelters, both underground and overground, personal and public are built across localities to safeguard people in case of emergencies—which is frequent and abrupt in that place. There is a national shift to prioritise safeguarding mass-scale lives and incur as minimal life loss as possible. There is an instinct amongst the populace to protect one's individual interests as well as population against external threats. Bunkers or Bomb Shelters then prove to be a very important asset for human life.

2. BACKGROUND

Our design approach is primarily based on IS 4991 (1968) – Criteria For Blast Resistant Design Of Structures For Explosions Above Ground (2), and IS 5499 (1969) – Code For Practice For Construction of Underground air-raid shelters in natural soil (3). In addition, the U.S. Air Force guidelines for blast-resistant construction have been taken into account – Air Raid Shelters in Buildings (US Office Of Civilian Defence) (4). Several academic theses and university research papers will also be referred to throughout the course of this project.

Before discussing the structural aspects of the bunker, it is necessary to first examine the nature of the blast loads it is designed to resist. That is, after all, its primary function—resisting the forces generated by explosions.

Blast loads are typically categorized into three types based on the magnitude of overpressure: low, medium, and high. Low overpressure ranges between 20–70 kPa and may cause damage to conventional structures but is often survivable. Medium overpressure spans 70–200 kPa and leads to severe damage, including structural collapse. High overpressure exceeds 200 kPa and causes complete structural failure, including underground effects.

We refer to the experimental observations of GI Taylor on blast wave propagation. A blast begins with a sharp rise in air pressure, followed by a shock front moving at supersonic speeds. This front decays over distance but can still deliver significant force. As the wave moves outward, it loses intensity, but depending on terrain and obstacles, it can reflect, refract, and focus, causing unexpected damage zones. Reflection off surfaces can amplify the pressure, and focusing—where curved shock fronts converge—can locally increase overpressure far beyond initial expectations.

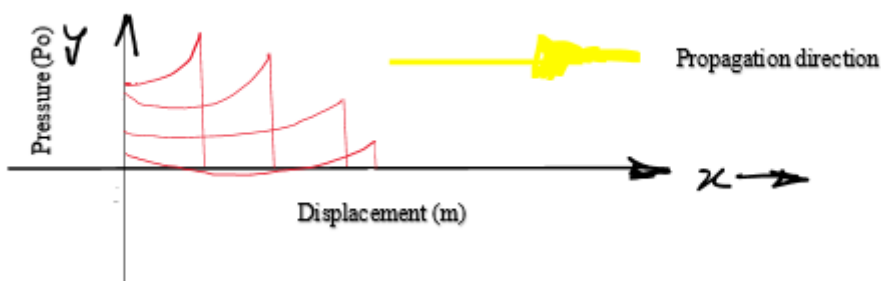


Fig 2.1 Propagation of a blast wave and its decay with time

Refraction, the bending of blast waves as they pass through different mediums or encounter variations in air density, further complicates the behavior. This can shift the direction of maximum impact away from the initial point of detonation, explaining why peripheral damage is often severe even when a structure is not the direct target.

Understanding all of these—initial pressure spike, wave speed, overpressure decay, thermal radiation, reflection, refraction, and focusing—is essential before we begin designing a structure that is supposed to withstand them.

When a blast wave hits a surface like the ground, it doesn't just reflect back. At certain conditions — usually when the blast is strong enough and the angle is shallow — something more serious happens. The reflected wave doesn't remain separate from the incident wave. Instead, they combine and form what's called a **Mach stem**. This merged wave is significantly more intense than either of the original two.

What you get is a triple point — the meeting of the incident wave, the reflected wave, and the newly formed Mach stem. This triple point moves outward, and the Mach stem essentially becomes a horizontal front of high-pressure air. The destruction it causes is not linear. It's amplified — well beyond what you'd expect just by calculating direct or reflected overpressures.

This makes it dangerous because structures that could've otherwise resisted a direct blast might collapse under the combined load. You also can't predict it easily — the Mach stem grows with time and distance from the source, and its size depends on the height of the blast, the surface it hits, and the strength of the explosion.

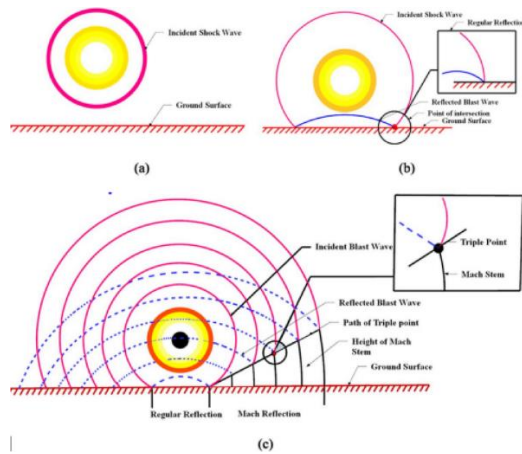


Fig 2.2 (a) Incident Waves (b) Reflection on hitting a solid surface (c) Mach Stem Formation [\(5\)](#)

That's why this concept became important — especially in the design of bunkers and hardened shelters. You design for regular blast pressure, but then this phenomenon comes in and doubles or triples the effective pressure without warning. So modern protective structures factor this in — consciously avoiding shapes and surfaces where Mach reflection is likely, or at least accounting for it in the material strength.

It's not some rare academic concept — this has real implications. People have seen entire reinforced structures fail because they didn't think a side-facing wall would ever see such high loads. But then a Mach stem formed, and it tore right through. Terror attacks are mostly localized, in congested urban areas, as they too tend to make use of **Mach Stem** formations, where even a small explosion would result into a greater damage on superposition with reflected waves and incoming waves, reflection would be extreme in congested regions, thus resulting in a greater **mach stem** and, hence, greater impact.

To understand the effect of a blast on any surface, we refer to a set of standardized parameters. They're fundamental to any simulation, theoretical calculation, or design check.

Charge Weight

This is the mass of the explosive material. Usually expressed in kilograms of TNT equivalent, because TNT is a global reference point. Every kind of explosion gets scaled to an equivalent TNT energy release. This number determines the initial power of the blast. A higher charge weight means higher peak overpressure and wider damage radius.

Standoff Distance

This is the physical distance between the blast center (point of detonation) and the point of interest or structure. It defines how the intensity of the wave will decay before it interacts with the target. The closer the standoff, the higher the overpressure.

Scaled Distance (Z)

This is where standardization begins. Scaled distance allows us to compare two blasts of different charge weights under the same framework.

The formula (2) is:

$$Z = \frac{R}{W^{\frac{1}{3}}} \quad \dots(2.1)$$

Where R is standoff distance, W is charge weight.

It neutralizes scale and lets you generalize findings across different explosives. It directly influences the predicted overpressure, impulse, and duration of the positive phase. Engineers use this to pull data from empirical charts or simulations and apply them to real cases. (1; 2)

Together, these three define the input conditions for any analysis of blast impact.

Obtaining the blast load:

We are going to use **Friedlander's equation** to formulate our blast load. This equation models the variation of overpressure with respect to time in a free-air blast. It's the standard form when you're dealing with idealized airburst explosions. The Friedlander equation is:

$$P(t) = P_0 \times \left(1 - \frac{t}{t_a}\right) \times e^{-\frac{\beta t}{t_a}} \quad \dots(2.2)$$

Where:

- $P(t)$ is the overpressure at time t
- P_0 is the peak overpressure
- t_a is the duration of the positive phase
- β is a decay constant (typically taken between 0.2 and 2 depending on empirical fit)
- e is the exponential decay base

This equation gives you a clean pressure-time history—starts at peak pressure P_0 at $t = 0$, linearly decays, and then exponentially drops off to atmospheric pressure. The graph looks like

a sharp triangle with a curved tail. For most engineering purposes, this curve can be simplified and approximated as a **triangular load**—starting from P_0 , linearly decreasing to zero at t_a . That simplification allows us to model dynamic pressure loads on structural elements without solving a nonlinear time function every time. We lose some realism, but for design and simulation, it's accurate enough.

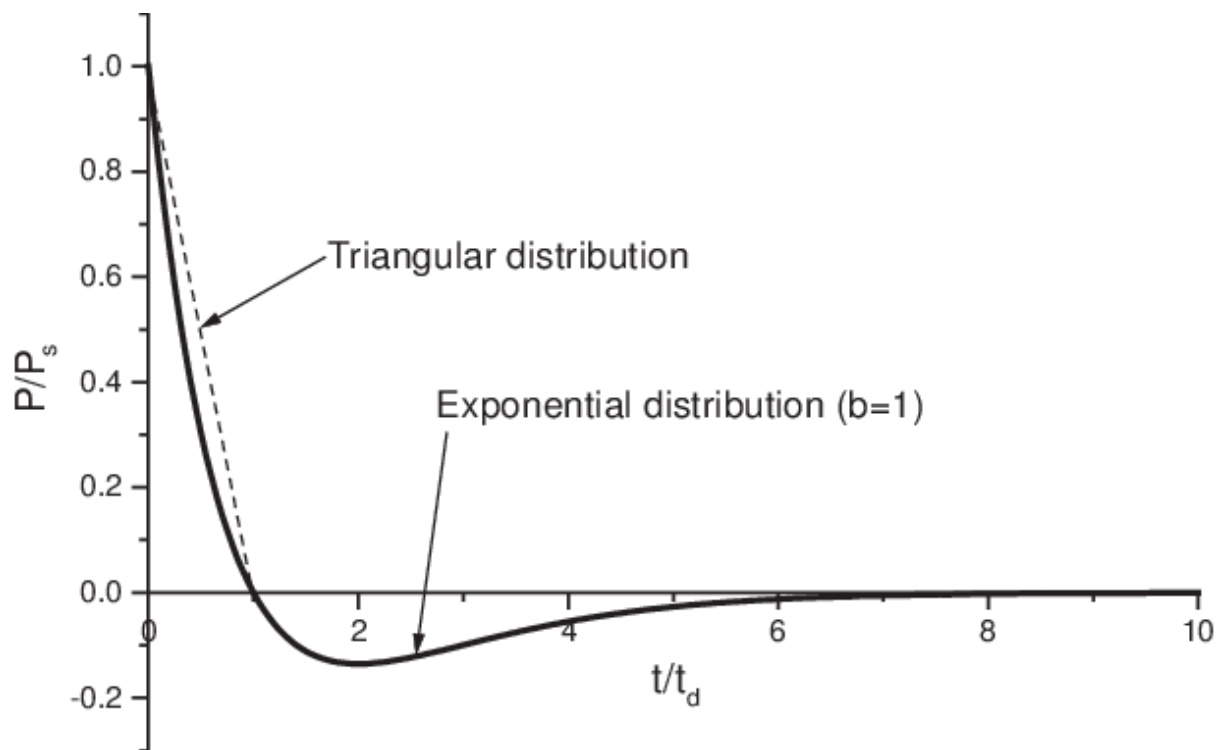


Fig 2.3 Triangular and Exponential Distribution of a blast load. We consider a triangular approximation for this purpose of calculating the blast load magnitude. [\(6\)](#)

It is suggested that the walls of a bunker should not be less than 300 mm in thickness [\(4\)](#), and the slope of the earthen cover must not exceed a 3/2 ratio [\(3\)](#). In standard military-grade construction, the wall thickness typically starts from 600 mm and goes beyond depending on the threat level. The maximum occupancy permitted in such structures is generally limited to 50 persons [\(3\)](#). For a single-room configuration, the minimum required height is set at 2 meters. [\(4\)](#)

Distance(m)	Peak side on Over Pressure	Mach Number M	Positive Phase Duration (ms)	Duration of Equivalent	Dynamic Pressure Ratio (qo/pa)	Peak Reflected over
-------------	----------------------------	---------------	------------------------------	------------------------	--------------------------------	---------------------

	Ratio (Po/Pa)			Triangular Pulse(ms)		pressure ratio
15	8	2.8	9.5	5.39	10.667	41.60
18	5	2.30	11.0	7.18	5.208	22.50
21	3.30	1.96	16.38	9.33	2.643	12.94
24	2.40	1.75	18.65	11.22	1.532	8.48
27	1.80	1.60	20.92	13.30	0.920	5.81
.
.
,

Table 2.1 Blast Parameters from Ground Burst of 1 Tonne Explosive ...IS 4991 (1968) Table 1. [\(2\)](#)

We are going to use Table 1 from IS 4991-1968 to obtain an approximate estimate of the amplitude of the dynamic overpressure generated by the blast wave at the ground surface. This value will be essential in evaluating the intensity of the blast load that the structure—specifically, the bunker—will be subjected to. Since the bunker is embedded beneath the soil, this surface overpressure provides a starting point to determine the transmission of the blast load through the soil medium and its subsequent effect on the buried structure.

Based on the literature surveyed and established engineering practices, the bunker design chosen for this project will follow the traditional vault-type configuration, consisting of two primary components: the cavern unit and the access tunnel. The cavern unit will serve as the main habitable or storage chamber, while the access tunnel will provide entry and exit to and from the structure. For design purposes, the dimensions of the cavern unit are assumed as follows: a length of 20 meters, a width of 15 meters, and a vertical wall height of 4 meters. On top of the walls, a curved arch of 2 meters is added, making the total internal height of the structure 6 meters at its apex. The access tunnel is planned to have a length of 10 meters, a width of 3 meters, and a height of 4 meters, maintaining consistency with standard movement and clearance requirements. [\(7\)](#)

These dimensions are assumed to be sufficient for accommodating personnel, equipment, and essential ventilation. This geometrical setup provides a simple yet effective form that has proven reliability in withstanding external pressure, especially under buried conditions.

3. METHODOLOGY

The Finite Element Method (FEM) stands in this modern times as one of the most powerful and versatile tools in computational engineering and science. It is a numerical technique for solving complex problems in civil engineering, structural mechanics, heat transfer, fluid dynamics, and electromagnetism—domains where analytical solutions are often impractical due to the intricacy of geometry, boundary conditions, or material behavior. At its core, the method transforms a complex physical problem into a discrete model composed of smaller, manageable parts called finite elements, over which equations can be approximately solved and then assembled into a global solution.

The origins of the finite element method can be traced back to the mid-20th century (around 1950s), when engineers and mathematicians independently developed discrete methods to analyze structures. Richard Courant, in 1943, provided the theoretical foundation using piecewise polynomial functions to approximate solutions to partial differential equations over triangular subdomains. However, it was not until the 1950s that the method began to take its modern form, particularly through the pioneering work of J.H. Argyris in aeronautics and Ray W. Clough in civil engineering, the latter of whom is credited with coining the term “finite element.” Courant's mathematical insight merged with the pressing engineering needs of post-war industry, and the method began to evolve into a formal procedure for analyzing stress in complex structures. The contributions of Olgierd Zienkiewicz further advanced the methodology, as he introduced a unified framework and comprehensive texts that helped popularize FEM within academia and industry alike. [\(1\)](#)

The real acceleration of FEM's application and importance came with the rise of computational power during the 1960s and 70s. As computers became capable of handling large systems of equations and memory-intensive tasks, FEM transitioned from a theoretical construct into a practical tool for solving real-world engineering problems. Programs like NASTRAN (developed by NASA), ABAQUS, ANSYS, and later COMSOL and LS-DYNA, allowed engineers across disciplines to simulate stresses, vibrations, heat flow, and even fluid–structure interaction with increasing accuracy. FEM thus became not just a method, but the backbone of modern computer-aided engineering. [\(1\)](#)

The basic methods of Finite Element Method includes the process of discretization—breaking down a continuous body into a finite number of subdomains or elements—and it is here that mesh generation plays a pivotal role. Meshing is the technique of subdividing a complex geometry into simple, non-overlapping regions where interpolation functions can be defined. These regions, or elements, may take the form of triangles or quadrilaterals in two dimensions, or tetrahedrons and hexahedrons in three dimensions. A well-constructed mesh ensures both geometric conformity and numerical stability; it captures the essential features of the physical domain while enabling the solution of governing equations with acceptable computational effort. A coarse mesh results in fewer equations and faster solution times but may lack precision, especially in regions with high gradients or discontinuities. Conversely, a fine mesh provides better accuracy but at the cost of computational efficiency.

Mesh generation is both an art and a science. Structured meshes are regular and grid-like, making them computationally efficient but often difficult to adapt to complex boundaries. Unstructured meshes, using irregularly shaped elements, are better suited to modeling intricate geometries and curved surfaces. In practical applications, hybrid meshing—combining both structured and unstructured regions—is often employed to balance efficiency and accuracy. The meshing process is typically aided by algorithms such as Delaunay triangulation or advancing front techniques, and more advanced solvers incorporate adaptive mesh refinement, which dynamically adjusts the mesh based on error estimators during the simulation. This adaptability is crucial when dealing with problems that involve large deformations, stress concentrations, or non-linear material behavior.

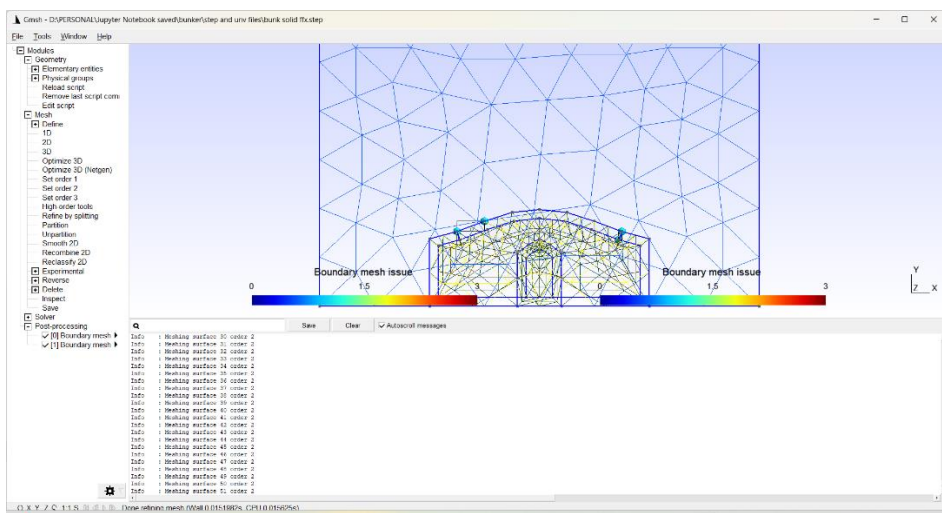


Fig 3.1 An example of meshing that was done on our blast-resistant bunker-soil compound using GMESH and refinements were further done using NETGEN. Since 3D Meshing was applied, the resultant was a mesh with Tetrahedron units.

One of the great strengths of FEM is its ability to handle highly complex shapes and boundary conditions that are otherwise intractable. With a sufficiently refined mesh and accurate element formulation, FEM can yield results that are remarkably close to experimental data, even for irregular geometries such as biological organs, aerospace structures, or geological formations. Its accuracy depends not only on the mesh but also on the choice of element type, integration scheme, and the physical models used. In high-fidelity simulations, FEM is capable of modeling phenomena across multiple scales and domains simultaneously—a task that would be virtually impossible using classical methods alone.

The development and advancement of FEM is a testament to interdisciplinary collaboration. From mathematicians like Courant, who provided the theoretical underpinning, to engineers like Argyris, Clough, and Zienkiewicz, who transformed it into a usable computational framework, the method reflects a convergence of ideas across fields. Today, FEM continues to evolve, with ongoing research in meshless methods, isogeometric analysis, and machine-

learning-based mesh optimization, all pushing the boundaries of what is computationally possible. As such, the finite element method is not just a numerical tool, but a foundational pillar of modern engineering analysis.

We begin by creating the geometry of the model using STAAD Pro, a modern tool for designing civil engineering structures. This geometry is then imported into FreeCAD, a free finite element software, where we define it as a solid and assign relevant material properties. We also model the surrounding soil compound. A three-dimensional mesh is then generated using basic tetrahedral elements. Finally, we use simulation tools such as CalculiX , Elmer FEM, Code_Aster, SimScale, etc. to run the finite element analysis.

3.1 FINITE ELEMENT METHOD

What is the Finite Element Method (FEM)?

The Finite Element Method (FEM) is a numerical approach used to solve problems governed by partial differential equations (PDEs) or those that can be expressed through functional minimization. It works by dividing the domain of interest into smaller subdomains called *finite elements*. Within each element, the physical field is approximated using interpolation functions defined by nodal values. This transforms a continuous problem into a discretized system where the nodal values are the primary unknowns. In the case of linear problems, this results in a system of linear algebraic equations. The values within the elements can then be computed using the nodal solutions.

Two key features of FEM include:

1. **Piecewise Approximation:** Even with simple interpolation functions, high accuracy can be achieved by increasing the number of elements.
2. **Locality:** The local nature of the approximation leads to sparse global matrices, enabling efficient solutions even for large-scale problems.

Working Principle of Finite Element Method:

Here is an outline of the general steps followed in FEM:

1. **Discretization:** The first step involves dividing the domain into finite elements. A mesh generator (preprocessor) creates arrays of nodal coordinates and element connectivities.
2. **Interpolation Functions:** Choose suitable functions (typically polynomials) to approximate the physical field within elements. The degree of the function depends on the number of nodes per element.
3. **Element Properties:** Derive the element matrix equations using methods like the variational principle or Galerkin method.

4. **Assembly:** Combine all element matrices into a global system using the connectivity data. Apply boundary conditions.
5. **Solution:** Solve the resulting system of equations, which is typically sparse, symmetric, and positive definite.
6. **Postprocessing:** Compute derived quantities (e.g., strains and stresses) from the solution.

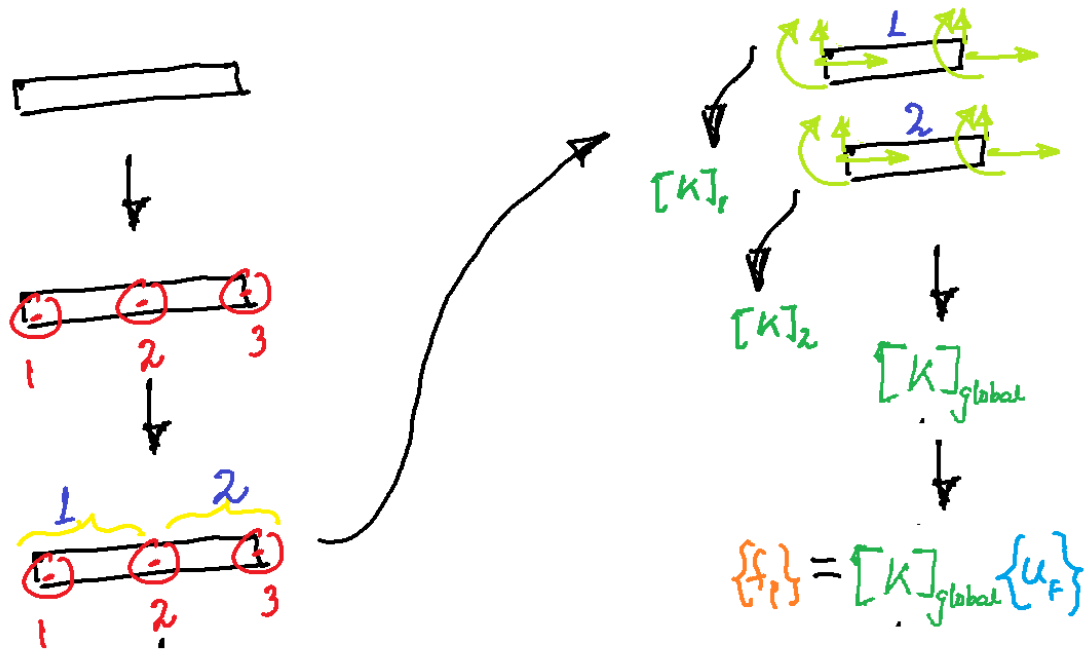


Fig 3.2 The Steps of Finite Element Method. It begins with A simple Bar element that is given three nodes in red, then discretized into two elements in blue, each assigned with Degree of Freedom (DOF), an element stiffness matrix $[k]$ is found out and each is merged to form a global $[K]$. Hooke's law is then applied.

Two-Dimensional Triangular Element ⁽⁸⁾

The triangular element is the simplest finite element, often used to introduce FEM concepts. For a triangle with three nodes, we use linear interpolation for displacements and :

$$\begin{aligned}
 u(x, y) &= N_1 u_1 + N_2 u_2 + N_3 u_3 \\
 v(x, y) &= N_1 v_1 + N_2 v_2 + N_3 v_3
 \end{aligned}
 \quad \dots(3.1)$$

The shape functions are linear and given by:

$$N_i(x, y) = \frac{1}{2\Delta} (a_i + b_i x + c_i y)$$

...(3.2)

Where:

$$a_i = x_{i+1}y_{i+2} - x_{i+2}y_{i+1},$$

$$b_i = y_{i+1} - y_{i+2},$$

$$c_i = x_{i+2} - x_{i+1}$$

$$\Delta = \frac{1}{2} (x_2y_3 + x_3y_1 + x_1y_2 - x_2y_1 - x_3y_2 - x_1y_3)$$

The strain-displacement matrix is:

$$[B] = \frac{1}{2\Delta} \begin{bmatrix} b_1 & 0 & b_2 & 0 & b_3 & 0 \\ 0 & c_1 & 0 & c_2 & 0 & c_3 \\ c_1 & b_1 & c_2 & b_2 & c_3 & b_3 \end{bmatrix}$$

...(3.3)

The elasticity matrix for plane problems is:

$$[E] = \begin{bmatrix} \lambda + 2\mu & \lambda & 0 \\ \lambda & \lambda + 2\mu & 0 \\ 0 & 0 & \mu \end{bmatrix}$$

...(3.4)

Where the Lamé constants are:

- **For plane strain:**

$$\lambda = \frac{\nu E}{(1 + \nu)(1 - 2\nu)}$$

...(3.5)

$$\lambda = \frac{\nu E}{1 - \nu^2}$$

...(3.6)

$$\mu = \frac{E}{2(1+\nu)}$$

...(3.7)

The stiffness matrix for the triangular element is:

$$[k] = \int_V [B]^T [E] [B] dV = [B]^T [E] [B] .$$

...(3.8)

Assuming unit thickness and constant matrices within the element, strains and stresses are also constant. [\(8\)](#)

Degree of Freedom (DOF) in FEM: [\(1\)](#)

A degree of freedom (DOF) is an independent value or parameter that defines the state or configuration of a system.

Each node in a finite element mesh can have one or more DOFs depending on the type of analysis. In 1D structural analysis: each node typically has 1 DOF (displacement in one direction). In 2D plane stress/strain problems: each node usually has 2 DOFs (displacements in x and y). In 3D solid mechanics: each node has 3 DOFs (displacements in x, y, and z). These DOFs are the unknowns that FEM solves for.

Example:

A 2D triangular element with 3 nodes and 2 DOFs per node will have a total of:

$$3 \text{ nodes} \times 2 \text{ DOFs per node} = 6 \text{ DOFs}$$

Convergence in FEM: [\(1\)](#)

Convergence in FEM refers to how the approximate solution approaches the exact solution as the mesh is refined. There are two main ways to achieve convergence:

1. h-convergence: decreasing the element size (making the mesh finer).
2. p-convergence: increasing the order of the interpolation polynomial (e.g., from linear to quadratic).

Convergence Criteria:

1. As mesh size or polynomial order , the FEM solution should:
 - o Satisfy the governing differential equations more closely.
 - o Show reduced error in displacement, strain, or stress fields.

Importance of DOF in Convergence:

2. Increasing DOFs (either by refining mesh or increasing interpolation order) usually improves accuracy.
3. But it also increases computational cost—so FEM aims to balance accuracy and efficiency.

3.2 MODEL SPECIFICATION

As mentioned in the literature (Refer to Background), the structural model we are designing will consist of two main components: a primary cavern unit and an adjoining access tunnel. The cavern, which serves as the main vault bunker, will be rectangular in plan with a length of 20 meters and a breadth of 15 meters. Its vertical walls will rise to a height of 4 meters. Above these walls, an arched roof—commonly referred to as a vault—will add an additional 2 meters to the total height, resulting in an overall internal height of 6 meters from the floor to the apex of the arch. This configuration not only provides ample storage or operational space within the bunker but also contributes to structural stability, especially under load conditions typically associated with underground or blast-resistant structures. [\(7\)](#)

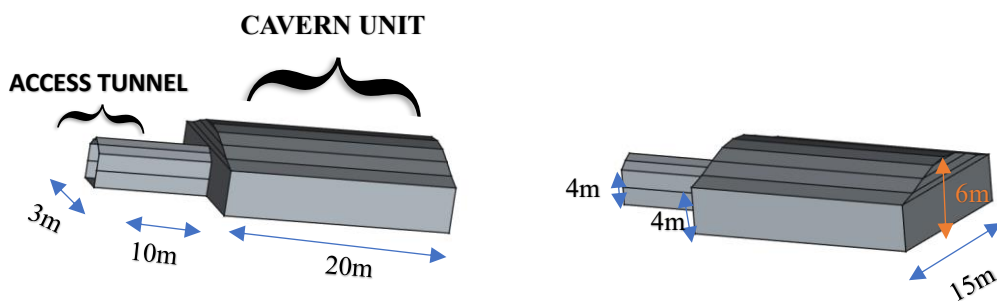


Fig 3.3 The Model Specifications Of Our Blast Bunker, from Table 3.1. Created using STAAD Pro 2014.

Adjacent to this primary chamber is the access tunnel, which is similarly designed with a vaulted cross-section. The tunnel will serve as a connecting or entry passage and is planned to be 10 meters long and 3 meters wide, with a maximum internal height of 4 meters at the crown of the arch. The use of a vault shape in both units is intentional, as it helps distribute stress more evenly and enhances the overall integrity of the underground construction. This dual-unit

design reflects both functional and safety considerations typical in secure civil infrastructure such as bunkers and subterranean facilities. [\(7\)](#)

	Length (m)	Breadth (m)	Wall Height (m)	Arch-Height (m)	Apex Height (m)
Cavern Unit	20	15	4	2	6
Access Tunnel	10	3	3	1	4

Table 3.1 The Model Specification Of our Blast Resistant Bunker. [\(7\)](#)

3.3 MODELING FROM GEOMETRY

We are going to use STAAD Pro 2014 for modeling and analyzing the bunker structure. STAAD Pro is a widely used structural analysis and design software that allows engineers to model structures like bunkers, silos, buildings, and bridges using a combination of graphical tools and a built-in code editor. The code editor is particularly powerful for precise control and customization. It lets us manually define joints (nodes), elements (such as beams, plates, or shells), supports (fixed, pinned, etc.), and loads (dead, live, wind, etc.). This flexibility helps in simulating complex geometries, such as our bunker with closed arched cardboard, which may not be easy to construct using the graphical interface alone.

The code used in STAAD Pro is written in a plain text format, typically saved with a .std extension. Since it is plain text, the file can be opened and edited using any text editor like Notepad, although STAAD Pro provides its own syntax-aware environment to avoid errors. This format allows for straightforward sharing, editing, and version control of models. Each section in the code—such as joint coordinates, element incidences, material specifications, and loads—is organized using clear keywords, making the model readable and modifiable. This makes it easier for us to document and replicate the structural setup of the bunker for both academic and professional purposes.

In the initial stage of the modeling process, we define the nodal coordinates that represent the geometric boundaries of the bunker structure. These nodes serve as key reference points in three-dimensional space and will subsequently be interconnected to generate the structural faces—walls, roof, and base—through shell and solid elements.

We define a .std Plain Text Code for it

STAAD SPACE

START JOB INFORMATION

ENGINEER

DATE 01-April-25

END JOB INFORMATION

INPUT WIDTH 79

UNIT METER KN

JOINT COORDINATES

1 0 0 0; 2 15 0 0; 3 15 4 0; 4 0 4 0; 5 15 0 20; 6 15 4 20;

7 0 0 20; 8 0 4 20; 9 1.875 4.5 0; 10 1.875 4.5 20; 11 3.75 5.2 0;

12 3.75 5.2 20; 13 5.625 5.8 0; 14 5.625 5.8 20; 15 7.5 6 0; 16 7.5
6 20; 17 9.375 5.8 0;

18 9.375 5.8 20; 19 11.25 5.2 0; 20 11.25 5.2 20; 21 13.125 4.5 0; 22
13.125 4.5 20; 23 6 0 0; 24 6 1.5 0;

25 6 1.5 -10; 26 6 0 -10; 27 6 3 0; 28 6 3 -10; 29 9 3 0; 30 9 1.5 0; 31 9 1.5 -10; 32 9 3
-10; 33 9 0 0; 34 9 0 -10; 35 6.75 3.6 0; 36 6.75 3.6 -10;

37 7.5 4 0; 38 7.5 4 -10; 39 8.25 3.6 0; 40 8.25 3.6 -10;

```
STAAD SPACE
START JOB INFORMATION
ENGINEER
DATE 01-April-25
END JOB INFORMATION
INPUT WIDTH 79
UNIT METER KN
JOINT COORDINATES
1 0 0 0;
2 15 0 0;
3 15 4 0;
4 0 4 0;
5 15 0 20;
6 15 4 20;
7 0 0 20;
8 0 4 20;
9 1.875 4.5 0;
10 1.875 4.5 20;
11 3.75 5.2 0;
12 3.75 5.2 20;
13 5.625 5.8 0;
14 5.625 5.8 20;
15 7.5 6 0;
16 7.5 6 20;
17 9.375 5.8 0;
18 9.375 5.8 20;
19 11.25 5.2 0;
20 11.25 5.2 20;
21 13.125 4.5 0;
22 13.125 4.5 20;
23 6 0 0;
24 6 1.5 0;
25 6 1.5 -10;
26 6 0 -10;
27 6 3 0;
28 6 3 -10;
29 9 3 0;
30 9 1.5 0;
31 9 1.5 -10;
32 9 3 -10;
33 9 0 0;
34 9 0 -10;
35 6.75 3.6 0;
36 6.75 3.6 -10;
37 7.5 4 0;
38 7.5 4 -10;
39 8.25 3.6 0;
40 8.25 3.6 -10;
```

Fig 3.4 The Code Editor in Utilities Section Of Staad Pro. The Nodes are defined there.

The nodes defined in the input are specific coordinate points in three-dimensional space that outline the geometric shape of the bunker and access tunnel. Each node is identified by a unique number and its corresponding X, Y, and Z coordinates (in meters), which indicate its position in the model. These nodes are used as anchor points to create structural elements such as walls, roof arches, and floor slabs. For example, nodes 1 to 8 form the rectangular prism of

the cavern walls, while nodes 9 to 22 define the arched vault roof by gradually increasing the Y-coordinate to create a curved profile.

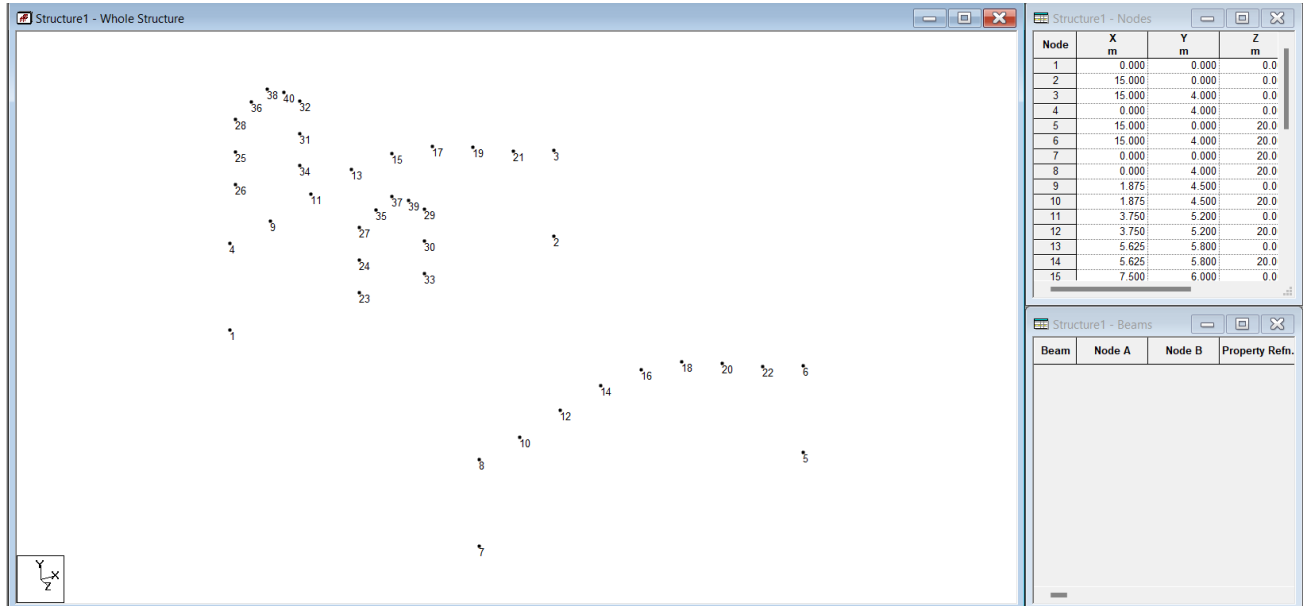


Fig 3.5 The Nodes are assigned for our models. This is their visual representation in the 3D coordinate plane

Now that the nodal coordinates have been established, the next step involves connecting these nodes using structural elements to form the physical surfaces—or "faces"—of the bunker and the access tunnel. These connections are made through the definition of *element incidences*, which specify how the nodes are grouped together to form different shell or plate elements that represent walls, roof arches, floors, and tunnel linings.

We begin by joining four nodes at a time to create flat quadrilateral surfaces, starting with the main cavern structure. For instance, elements 1 to 5 connect nodes 1 through 7 in a sequence that forms the floor and vertical walls of the bunker. As we move on, the curved roof structure is modeled by gradually connecting higher-elevation nodes—such as nodes 9 to 22—which simulate the rise of the vault arch across the bunker's length. These segments form the vaulted roof through a series of shell elements, mimicking the curvature using straight-sided plates arranged in an arc.

Similarly, the access tunnel is constructed using another set of nodes and shell elements. Nodes are placed in a manner that outlines the tunnel's arched profile, and elements 14 to 22 use these coordinates to construct the tunnel floor, walls, and roof. Through this process of connecting nodes with elements, we assemble a complete 3D representation of the bunker and its tunnel in STAAD, laying the foundation for further analysis such as stress distribution, displacement, and load handling.

First, we begin forming the surfaces of the bunker by joining specific sets of four nodes to create shell elements, which represent walls and floors. For instance, by connecting nodes 1, 4,

8, and 7, we define one of the vertical side walls of the cavern. This quadrilateral forms a flat surface representing the outer face of the bunker.

Following a similar method, we create adjacent walls and surfaces by carefully selecting and linking the relevant nodes. For example, the nodes 8, 6, 5, and 7 are joined to construct the opposite side wall of the bunker. The set of nodes 6, 3, 2, and 5 forms the front wall, while nodes 1, 2, 5, and 7 complete the base or floor of the structure. By successively forming these quadrilateral shells using the defined node positions, we gradually build the main volume of the bunker in the form of vertical walls and a flat base. Each group of four nodes defines a planar surface, and collectively they establish the geometric boundaries of the underground structure.

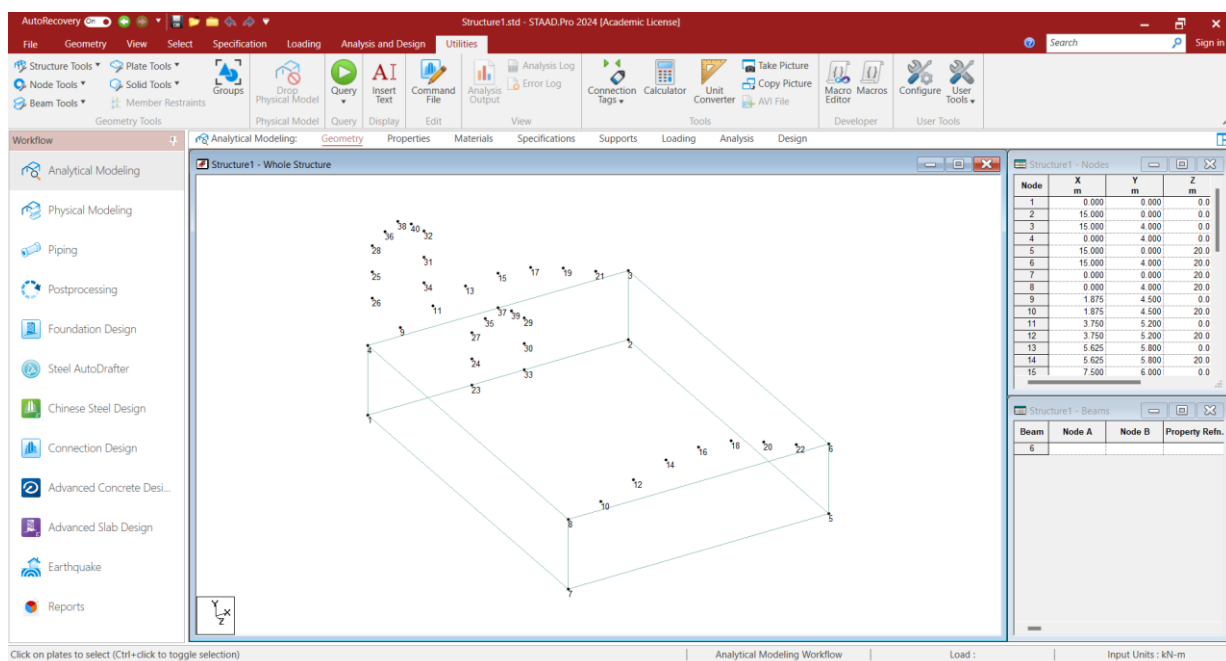


Fig 3.6 The nodes that would form the room of our cavern unit are joined to form a quadrilateral shell structure. Staad Pro 2014 was used.

Staad Pro Code Editor Plain Text (.std file)

ELEMENT INCIDENCES SHELL

```
1 1 2 3 4;
2 2 5 6 3;
3 5 7 8 6;
4 7 1 4 8;
5 1 2 5 7;
```

Now we begin constructing the vaulted (arched) roof structure of the bunker by connecting specific nodes in sequence to form shell elements, each representing a curved segment of the vault. This process involves layering plates step by step from one side of the bunker to the other, following the curvature of the vault.

We start by connecting nodes 4, 9, 8, and 10 to form the first shell plate of the arch, which serves as the base of the vault near one wall. Next, we move slightly upward and inward along the curvature, joining nodes 9, 11, 12, and 10 to form the next shell segment. Continuing this progression, we connect nodes 11, 13, 14, and 12 to extend the vault further.

The pattern continues with nodes 13, 15, 16, and 14, followed by nodes 15, 17, 18, and 16, and then nodes 17, 19, 20, and 18. Each of these connections forms a flat shell plate that approximates a segment of the curved roof. By carefully sequencing the node connections along the parabolic or circular profile, we simulate the shape of an arch using planar shell elements in the model. This approach allows the STAAD software to analyze the structure realistically while maintaining computational simplicity.

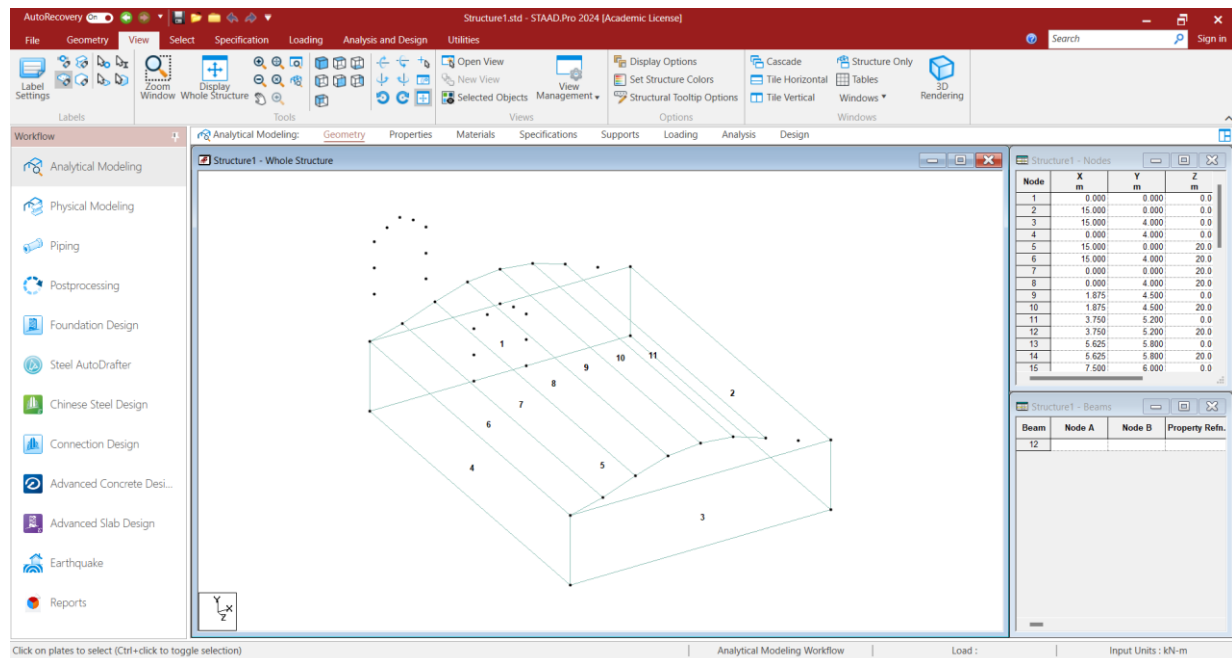


Fig 3.7 The Vault is being made by joining the nodes. The plate numbers are being shown.

The following plain text command makes the shell for the vault. Refer to the Plate numbers in Fig 3.7 to get a better idea of the code: how the nodes were joined

6 4 9 10 8;

7 9 11 12 10;

8 11 13 14 12;

9 13 15 16 14;

10 15 17 18 16;

11 17 19 20 18;

After constructing the central arch plates of the vault, we complete the vault structure by joining the remaining nodes to close the arch at the far end. Specifically, we connect nodes 20, 19, 21, and 22 to form a rectangular shell segment, and then join nodes 22, 21, and 3, 6 to create another rectangular plate. These two triangular shells serve to smoothly taper and close the curved roof at the opposite end of the vault.

With these final shell elements added, the arched roof is now fully enclosed and securely rests atop the quadrilateral shell structure that forms the main rectangular room of the bunker. This combination of planar wall shells and a vaulted roof allows for a realistic simulation of the bunker geometry and its structural behavior under load.

Additional Code in the code editor of the Staad pro:

12 19 21 22 20;

13 21 3 6 22;

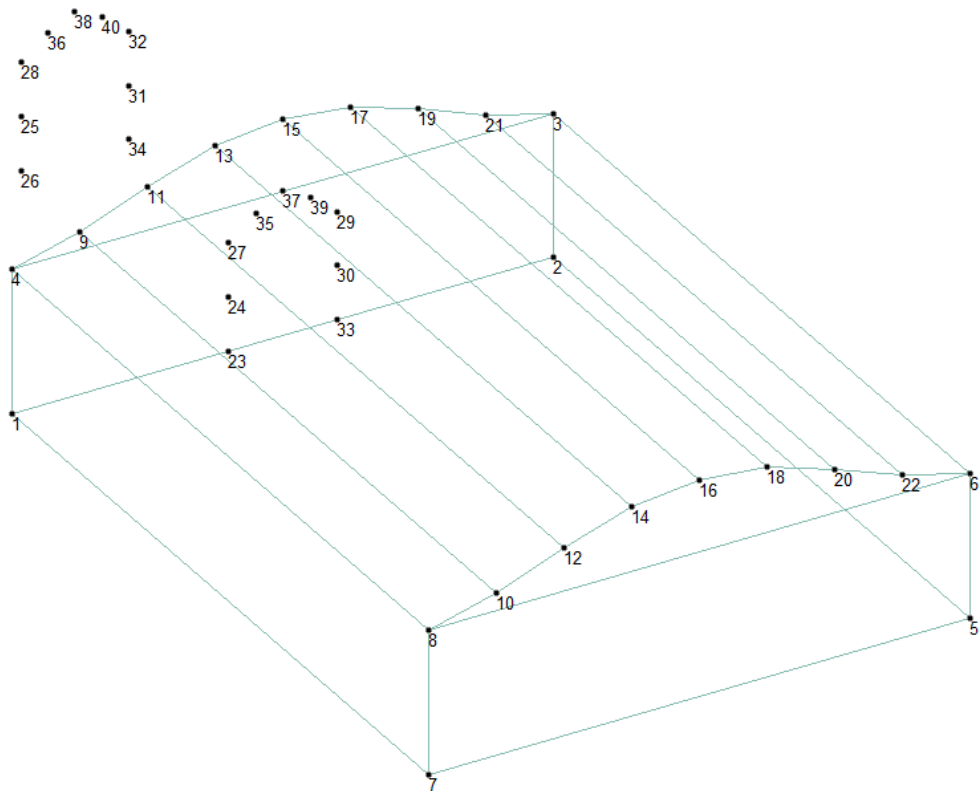


Fig 3.8 Now our arch vault plate is ready.

Now, we proceed to construct the access tunnel by referring to the specific nodes already assigned to represent its geometry. The access tunnel, being a separate structural unit, also follows a vault-like shape and consists of vertical walls and a curved roof section.

To begin with, we create the side walls of the tunnel. For the first wall, we connect nodes 26, 25, 24, and 23 to form a rectangular shell, representing the base portion. Then, directly above it, we join nodes 25, 28, 27, and 24 to form the upper extension of the same wall. This stacked configuration gives the wall its full height and continuity.

Similarly, for the opposite wall of the tunnel, we form the base by joining nodes 34, 31, 30, and 33. Just above this, we connect nodes 31, 32, 29, and 30 to construct the upper portion. These two walls now define the lateral boundaries of the access tunnel and provide the support needed for the arched roofing that will follow.

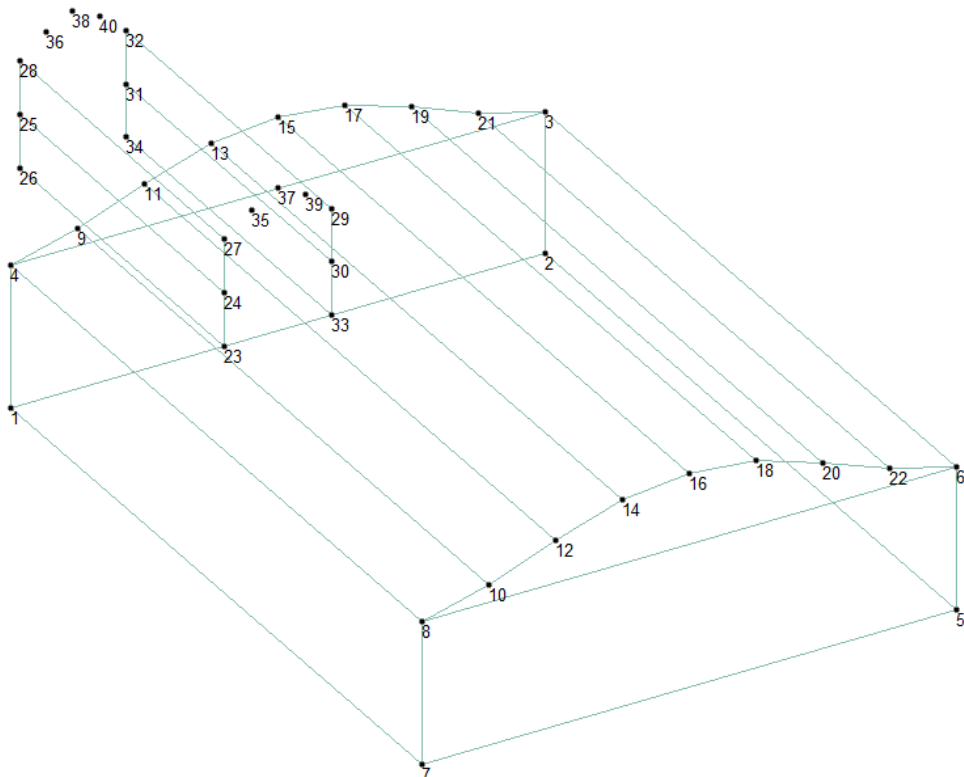


Fig 3.9 The Making of the Access Tunnel wall.

The Staad plain text code will be:

14 23 24 25 26;

15 24 27 28 25;

16 29 30 31 32;

17 30 33 34 31;

Next, we define the vault—or the curved arched roof—of our access tunnel by systematically connecting the nodes that trace its vault geometry. This vault segment forms the top enclosure and gives the tunnel its distinct profile.

We begin by forming the first shell of the arch by joining nodes 28, 36, 35, and 27. Then we move upward to the next shell, joining nodes 36, 38, 37, and 35. This continues with another plate formed by connecting 38, 40, 39, and 37. Finally, the arch is completed by connecting the last segment using nodes 40, 32, 29, and 39. Together, these shells form the continuous arched roof over the access tunnel, thus enclosing the structure and giving it its definitive, vaulted appearance.

Additionally, we complete the definition of the tunnel unit by assigning its base or floor. This is done by connecting nodes 26, 34, 33, and 23. This rectangular plate represents the ground surface of the tunnel, providing structural closure and completing the overall tunnel geometry. With the floor in place and the arch overhead, the access tunnel is now fully defined as a governed structural unit.

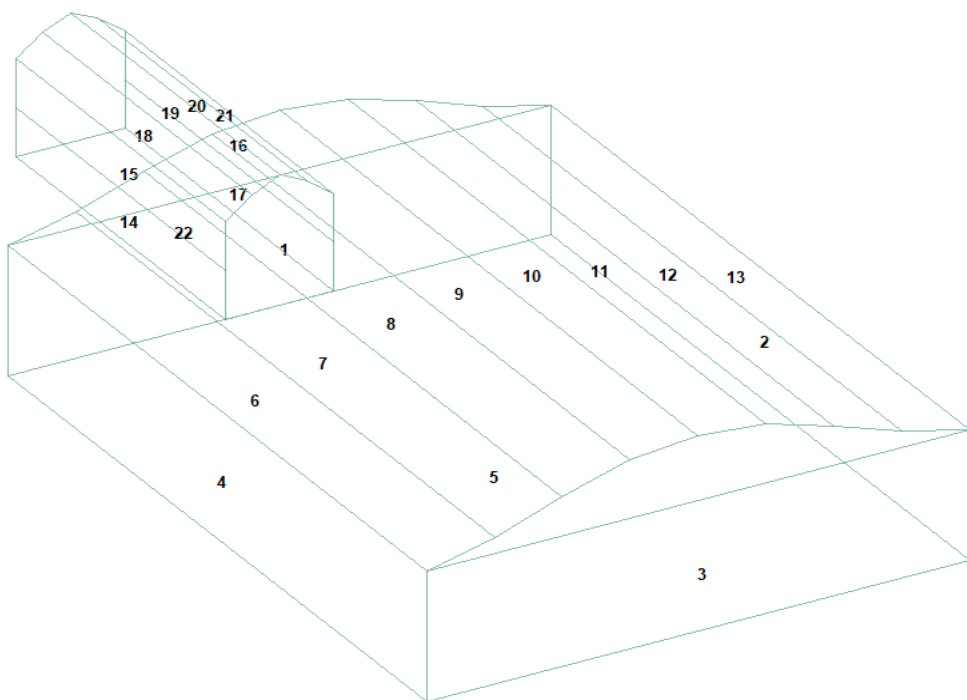


Fig 3.10 The Shell Of Our Bunker with the assigned Plate numbers.

Hereby we have our staad pro command:

18 27 35 36 28;

19 35 37 38 36;

20 37 39 40 38;

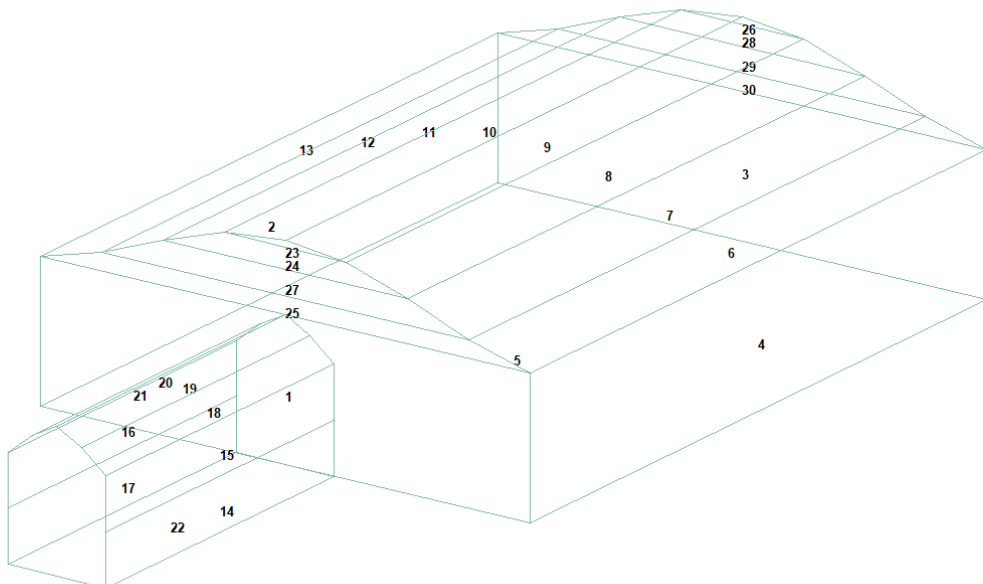
21 39 29 32 40;

22 23 33 34 26;

Now comes a crucial final step in completing our bunker model. Between the vault's arched roof and the vertical walls of the structure, there remains a transitional space—an open gap that, if left undefined, would result in an incomplete shell and compromise the integrity of the model. To close this space and ensure the bunker behaves as a monolithic structure under analysis, we introduce additional plates.

Specifically, we define shell elements by connecting the following nodes to enclose these transitional regions: 23, 24, 25, 26, 27, 28, 29, and 30. These nodes trace the vertical and curved transition between the vertical walls and the vaulted ceiling of the access tunnel.

By defining shell elements on both the front and rear faces using these nodes, we seal off the structure completely. This transforms our model into a fully enclosed shell system, ensuring that it responds realistically to loading conditions and behaves as a structurally coherent unit during analysis.



Y,

Fig 3.11 The surface is finally closed as plates 23,24,27,25 and 26,28,29,30 are defined to fulfil both the sides.

This is our final plain text description of plates in staad.

23 13 15 17;

24 11 13 17 19;

25 4 9 21 3;

26 14 16 18;

27 9 11 19 21;

28 12 14 18 20;

29 10 12 20 22;

30 8 10 22 6;

FINISH

Thus, the shell structure defined using nodes and plates is exported as a DXF file, which serves as a geometric framework for further analysis. This DXF file can be imported into any compatible finite element software, where the shell model acts as the foundational geometry for creating a solid structure. By extruding or meshing the shell into a 3D solid, the software enables us to define material properties, loading conditions, and boundary constraints necessary for finite element analysis (FEA). Once the solid model is prepared, we perform FEA to study the structural behavior of the bunker—such as stress distribution, deformation patterns, and safety under different loading scenarios—ultimately allowing us to evaluate the performance and integrity of the design.

This is our entire plain text code that was used in the code editor of Staad pro 2014 under Utilities that sets our entire geometry:

```
STAAD SPACE DXF Import of bunker with closed arched cardboard
START JOB INFORMATION
END JOB INFORMATION
INPUT WIDTH 79
UNIT METER KN
```

JOINT COORDINATES

```
1 0 0 0; 2 15 0 0; 3 15 4 0; 4 0 4 0; 5 15 0 20; 6 15 4 20; 7 0 0 20;
8 0 4 20; 9 1.875 4.5 0; 10 1.875 4.5 20; 11 3.75 5.2 0; 12 3.75 5.2 20;
13 5.625 5.8 0; 14 5.625 5.8 20; 15 7.5 6 0; 16 7.5 6 20;
17 9.375 5.8 0; 18 9.375 5.8 20; 19 11.25 5.2 0; 20 11.25 5.2 20;
21 13.125 4.5 0; 22 13.125 4.5 20; 23 6 0 0; 24 6 1.5 0; 25 6 1.5 -10;
26 6 0 -10; 27 6 3 0; 28 6 3 -10; 29 9 3 0; 30 9 1.5 0; 31 9 1.5 -10;
32 9 3 -10; 33 9 0 0; 34 9 0 -10; 35 6.75 3.6 0; 36 6.75 3.6 -10;
37 7.5 4 0; 38 7.5 4 -10; 39 8.25 3.6 0; 40 8.25 3.6 -10;
```

ELEMENT INCIDENCES SHELL

```
1 1 2 3 4; 2 2 5 6 3; 3 5 7 8 6; 4 7 1 4 8; 5 1 2 5 7; 6 4 9 10 8;
7 9 11 12 10; 8 11 13 14 12; 9 13 15 16 14; 10 15 17 18 16;
11 17 19 20 18; 12 19 21 22 20; 13 21 3 6 22; 14 23 24 25 26;
15 24 27 28 25; 16 29 30 31 32; 17 30 33 34 31; 18 27 35 36 28;
19 35 37 38 36; 20 37 39 40 38; 21 39 29 32 40; 22 23 33 34 26;
23 13 15 17; 24 11 13 17 19; 25 4 9 21 3; 26 14 16 18; 27 9 11 19 21;
28 12 14 18 20; 29 10 12 20 22; 30 8 10 22 6;
```

FINISH

3.4 SOLID PROPERTIES

Since Abaqus limits the number of nodes for our FEM purpose available under its free tier upto only 1000 nodes, we opt for an alternative approach using the open-source CAD platform FreeCAD for our finite element analysis. FreeCAD offers a flexible environment for mesh creation and solid modeling without node restrictions. To proceed, we upload the previously exported DXF file—containing our defined shell structure—into FreeCAD. This shell model, once imported, will serve as the geometric basis for defining a 3D solid. Within FreeCAD, we will convert the shell into a solid body by closing the surfaces and extruding or thickening where necessary. This transformation enables us to run a complete structural simulation directly in FreeCAD using its built-in FEM workbench, thereby bypassing Abaqus limitations while ensuring detailed analysis of our bunker design.

First, we perform an **extrusion** operation on the shell model. Extrusion is a process in computer-aided design (CAD) where a 2D surface or shell is extended linearly along a specified direction to generate a 3D volume. In our case, each shell plate—essentially a flat surface defined by four nodes—is extruded to a certain thickness, effectively turning it into a solid plate.

By extruding all the plates one by one, we begin to create volumetric elements that represent the actual thickness of the bunker walls, arch, and access tunnel. These extruded volumes join together edge-to-edge and face-to-face. While they may appear to intersect at some boundaries, they are not overlapping improperly—rather, they share common edges or surfaces, forming a closed and connected solid geometry. This interconnected structure is essential for accurate finite element analysis, as it allows the simulation software to understand load paths and material continuity across the entire model.

Each plate in our bunker model will be extruded by 600 mm (approximately 24 inches), aligning with standard practices for reinforced concrete structures. This thickness is commonly adopted for load-bearing walls in residential and commercial buildings, providing sufficient strength and durability under various loading conditions .

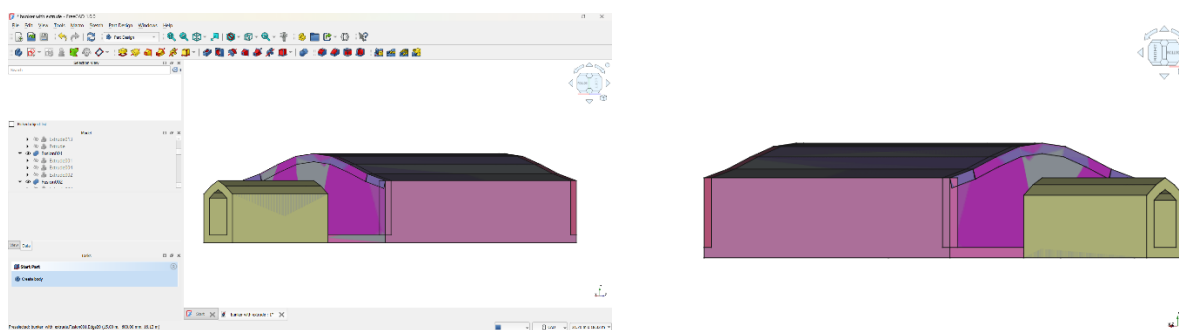


Fig 3.12 The final extruded plates of the bunker model. The extrude option is available in Part workbench of FreeCAD

In FreeCAD, we will extrude each shell plate by 600 mm to transform the 2D surfaces into 3D solid elements. This process effectively imparts the necessary thickness to the walls, converting

our shell model into a volumetric representation suitable for finite element analysis. The extrusion ensures that each wall segment possesses the structural integrity required to withstand anticipated loads, such as soil pressure and environmental forces.

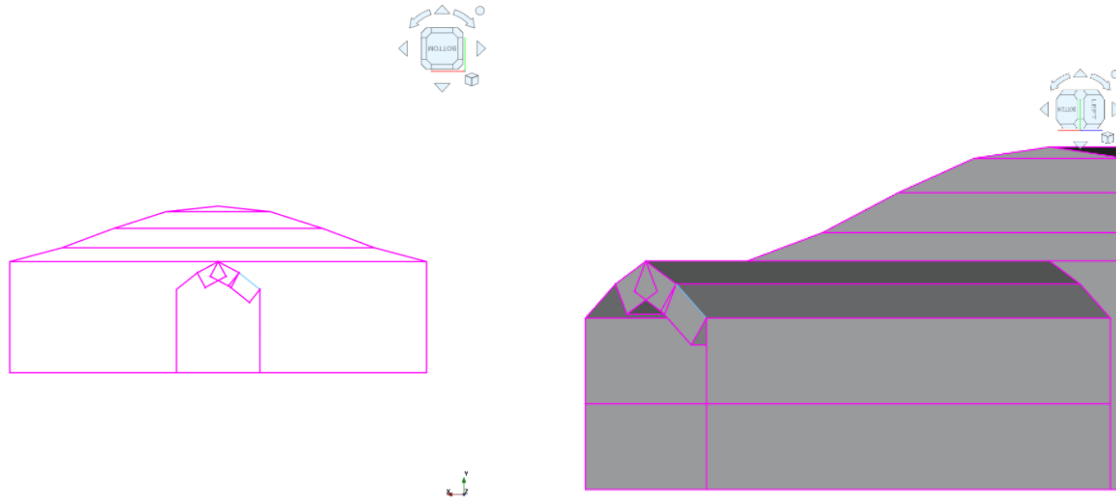


Fig 3.13 The shell plates that form the vault of the access tunnel are extruded here. As you can see, a thickness of 600mm is introduced. And they merge with each others, thus, it will be easy to fuse them later.

By adhering to this standard wall thickness, we ensure that our bunker model is both structurally sound and compliant with typical construction norms. This approach facilitates accurate simulation of the bunker's performance under various scenarios, providing valuable insights into its safety and reliability.

We will eventually extrude every plate in our bunker model by 600 mm, which is the intended wall thickness based on standard reinforced concrete practices. Refer to Fig 3.14. This extrusion process is done using the Extrude command found in the Part Workbench of FreeCAD. When we apply the extrude operation to a shell or surface, it creates a volumetric shape by stretching the 2D surface along a given direction—essentially thickening the surface into a prism-like body. As a result, each plate or shell in the bunker becomes a visually solid-like component, now having depth in addition to length and breadth.

However, it's important to understand that extrusion alone does not automatically create a true solid body in the engineering or simulation sense. Instead, each extruded shell remains a standalone volumetric part—like individual hollow pipes or boxes—that are not yet fused into a single, unified solid structure. In fact, since we are extruding each of the approximately 30 shell plates separately, what we get in the end are 30 distinct volumetric bodies sitting together, side-by-side or intersecting, but not yet merged into a single continuous mass.

Therefore, while extrusion gives us volume, it does not give us solidity or structural unity. To convert this collection of extruded components into a cohesive solid body—something that can be analyzed reliably in finite element analysis—we need to take additional steps. These typically include using Boolean operations such as Union (Fuse) or Part → Make Compound in FreeCAD, which allow us to combine all the extruded bodies into a single, unified solid. Only after this process can our bunker model be treated as one complete solid

object, ready for meshing and simulation. Until then, the structure remains a group of separate components that merely appear to form a bunker.

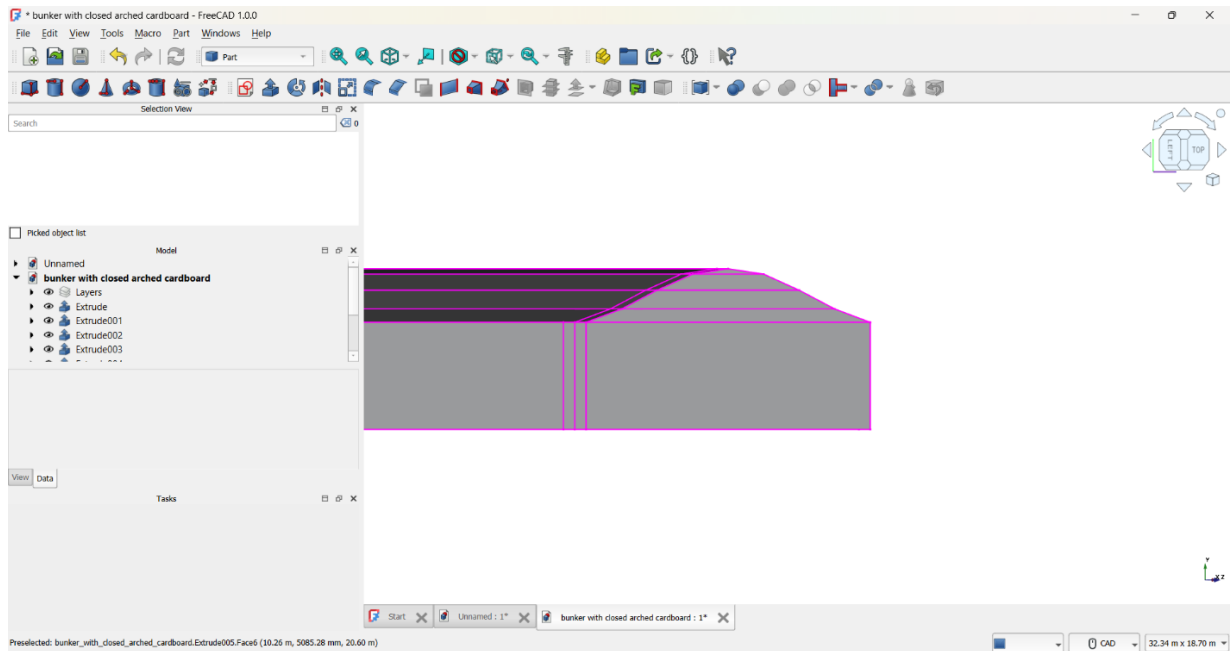
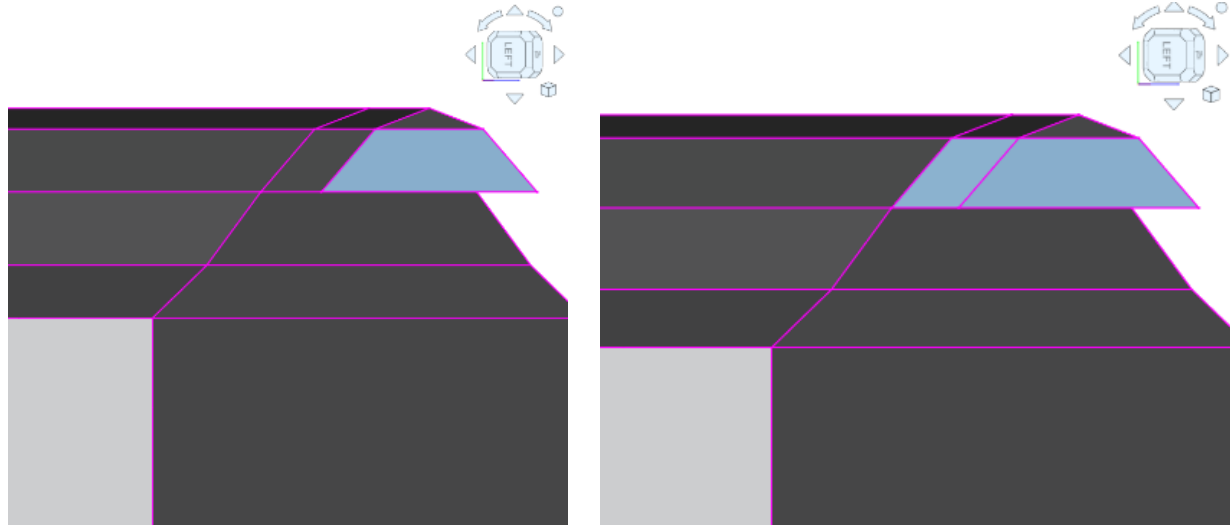


Fig 3.14 The extrude of 600mm being applied to the plates at the rear end. Look how they have thickened and merged with the neighbor extrusions at the edge.

Handling each extrusion individually can become tedious and inefficient, especially when working with complex structures like our bunker, which consists of around 30 separate plates. Thus we will have 30 separate extrusions and handling them would be very difficult. To manage all these extruded components more effectively in FreeCAD, we use a tool called Compound.

What is a Compound?

In FreeCAD, a Compound is a type of grouped object that combines multiple separate bodies (such as extruded shells) into one manageable unit without altering their individual identities or geometry. Think of it like placing several objects into a single box—you can move, rotate, and apply operations to the entire group all at once. The Compound does not merge the parts into a single solid; it just keeps them bundled for ease of handling. This is particularly helpful when preparing to perform collective operations like Boolean unions, ensuring that all components are treated together without manually selecting them one by one.

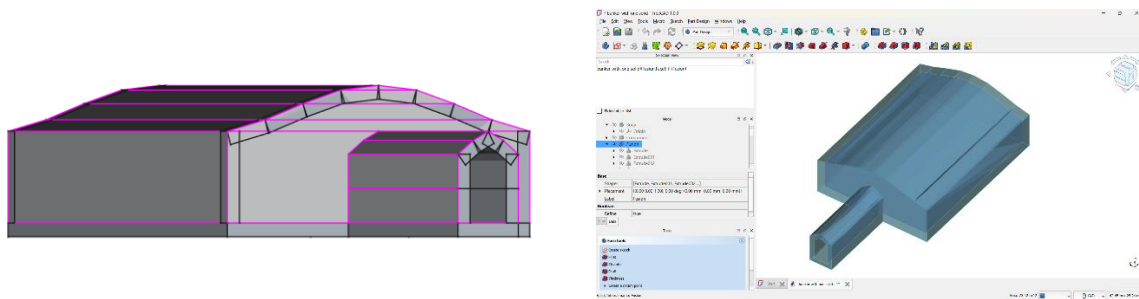


Fig 3.15 The final extrude model with 30 solids and the boolean fused union with one solid.

On performing a Check Geometry operation in the part workbench on our compound of extrudes, we get the following results:

Checked Object	Compound
Shape Type	Compound
Vertices	240
Edges	358
Wires	179
Faces	179
Shells	30
Solids	30
Compounds	1
Shapes	1017
Area (mm ²)	2733383733.41
Volume (mm ³)	523219850349.72
Length (mm)	3978046.69
Global Placement	placement

Table 3.2 The Check Geometry results of the Compound that contains our extrudes.

After creating a compound, we can move to the next important step: Boolean Fuse, also known as Union. This is found in the Part Workbench under Boolean operations. Boolean Fuse is a function that permanently combines multiple solid bodies into a single, unified solid. It checks for intersecting volumes between parts and merges them into one continuous structure. Unlike the Compound, which only groups bodies, the Boolean Fuse physically connects them—

removing overlapping interiors, joining touching faces, and creating one single solid object that behaves as a unified whole during simulations or further modeling steps.

In our case, we'll first extrude all shell plates by 600 mm, then collect them into a Compound. Once grouped, we'll use Boolean Fuse to merge this collection into a true solid bunker. This final fused structure is what we'll use for meshing and finite element analysis.

On performing a Check Geometry operation in the part workbench on our fusion of that compound, we get the following results:

Checked Object	Fusion
Shape Type	Compound
Vertices	80
Edges	120
Wires	46
Faces	45
Shells	2
Solids	1
Compounds	1
Shapes	295
Area (mm ²)	2733383733.41
Volume (mm ³)	523219850349.72
Length (mm)	3978046.69
Global Placement	placement

Table 3.3 The Check Geometry results of the Fusion that was made by using Boolean fusion operation on our compound that contained the extrudes.

Now that we have a fused singular solid of our bunker, it exists only as a geometric form—a closed 3D volume with shape but no physical identity. At this stage, the model is purely abstract. It could represent wood, plastic, emerald, or even silk, and the simulation software would not differentiate. This is why assigning material properties is a critical next step. To make this model physically meaningful and ready for finite element analysis (FEA), we must define the real-world materials it represents.

For bunker structures, RCC (Reinforced Cement Concrete) is the most appropriate choice due to its excellent compressive strength, durability, and resistance to blasts and environmental factors. RCC combines concrete for compressive strength and steel reinforcement for tensile capacity. We're going to simulate this bunker as constructed with RCC of grade M30 or M35.

M30 indicates that the concrete mix has a characteristic compressive strength of 30 MPa (megapascals) after 28 days of curing. M35 offers a slightly higher strength of 35 MPa, suitable for more demanding load-bearing applications, such as bunkers, retaining walls, and bridges.

These properties can be input into your simulation software under the material definition settings, depending on whether you're using linear static analysis or more advanced simulations. In FreeCAD, you can define these materials under the material editor or during meshing and simulation setup via the FEM Workbench.

By assigning RCC properties, we transition from abstract geometry to a physically meaningful model that accurately reflects real-world behavior, enabling meaningful structural analysis.

Density (kg m ⁻³)	2550
Young's Modulus Y (Pa)	30×10^9
Poisson Ratio	0.22

Table 3.4 The material properties of RCC used when we choose M30 Grade of Concrete and Fe415 grade of Steel [\(1\)](#) [\(9\)](#)

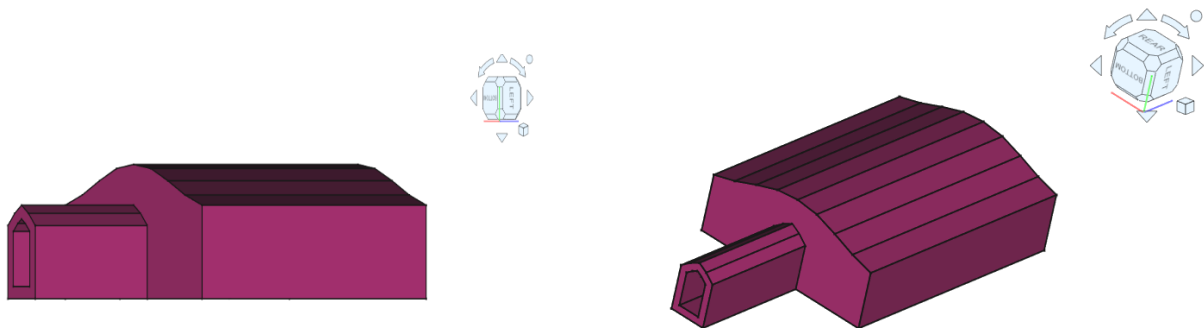


Fig 3.16 The final solid bunker as one complete fused solid. These are two views of the same.

3.5 SOIL PROPERTIES

Now that we have our bunker ready as one singular solid, the next essential step is to define the surrounding soil mound, because our bunker is designed to be underground, embedded within a protective cover of soil. This soil mound is not only important for realism in the finite element simulation but also crucial for load transfer, thermal insulation, and blast resistance.

We will create a larger volume surrounding the bunker geometry, representing the soil, with a defined depth above and around the bunker. This soil block should ideally extend at least 2–3 times the dimensions of the bunker in each direction to allow accurate simulation of pressure distribution, settlement, and load-bearing behavior.

In FreeCAD, we will model the soil mound as a separate solid body, often a cuboid or hemispherical mass depending on terrain assumptions. The soil and the bunker will be

assigned different material properties, and their interaction (contact or embedded condition) will be defined during analysis.

For our purpose, we are going to define the soil mound using the Cube feature in FreeCAD, representing the mass of earth that encloses the underground bunker. The cube will have dimensions of 30 meters in breadth (x), 20 meters in depth (y), and 70 meters in length (z), making it large enough to simulate realistic underground pressure and environmental conditions.

To correctly position the bunker within this soil mound, we'll adjust the cube's placement in the 3D coordinate system:

- The X-coordinate will range from -7.5 meters to 22.5 meters, centering the bunker in the X-direction so that our aim is clear.
- The Y-coordinate will range from -0.6 meters to 19.4 meters, placing the bunker about 15.4 to 13.4 m below the surface, which is a reasonable depth for both protective cover and structural simulation.
- The Z-coordinate will range from -10 meters to 60 meters, placing the bunker such that the entrance of the access tunnel meets at one edge of the bunker. It can be said that the bunker is in the far end of the soil mound where it meets its opening, thus also allowing ventilation for that purpose.

This positioning ensures that the bunker remains centrally embedded, while the access tunnel reaches the edge of the soil block, simulating a realistic entry point in terrain.

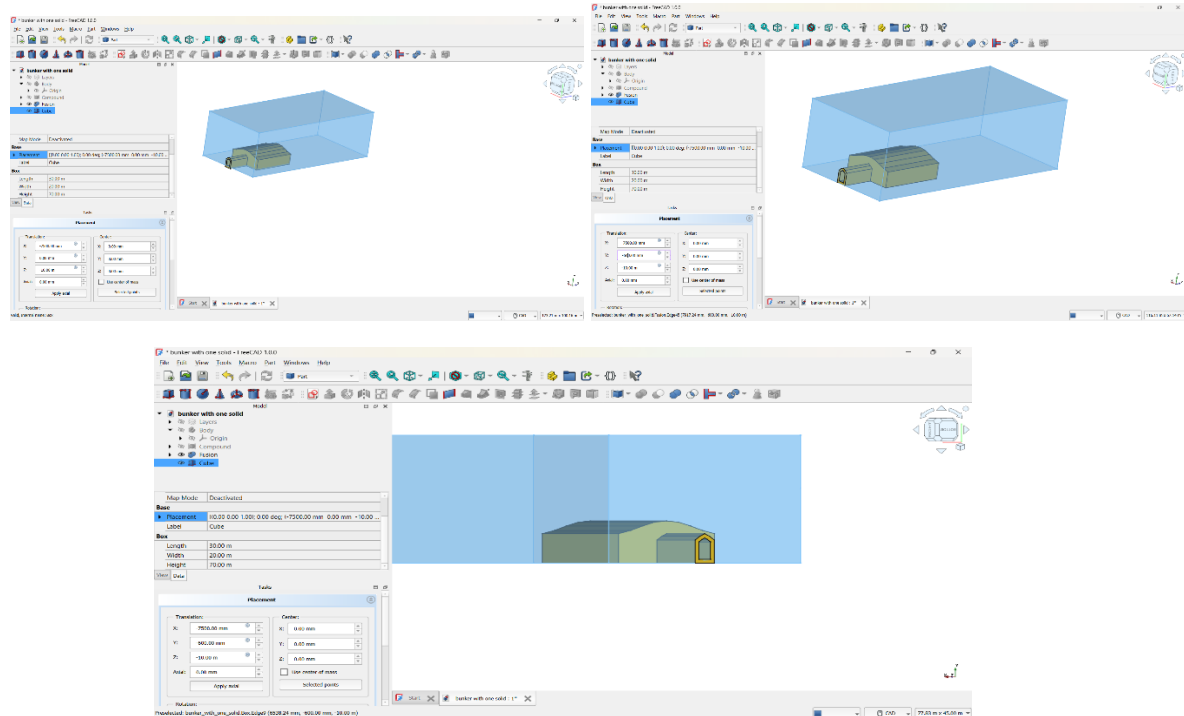


Fig 3.17 The bunker embedded within the soil mound.

We have carefully selected the dimensions of the soil mound based on conventional and widely accepted military engineering standards for blast-resistant structures. The depth of 20 meters is chosen because military-grade underground bunkers are typically buried between 10 to 25 meters deep to effectively attenuate shock waves from surface or aerial explosions. A greater depth allows the soil mass to absorb and dissipate more of the incoming energy, reducing the stresses transmitted to the bunker walls. [\(4\)](#)

The length of 70 meters is selected to ensure adequate distance from the blast origin to the structure, as we will later apply blast loads at specified standoff distances. This helps us simulate realistic scenarios where explosives are detonated at some distance from the bunker surface, allowing for a gradual distribution of stress waves through the soil.

The breadth of 30 meters serves two purposes: it centers the bunker within the mound for uniform coverage and ensures that lateral soil pressure and confinement are balanced on either side. These dimensions represent safe design thresholds to ensure that the bunker remains protected, stable, and minimally affected by the blast loads during finite element analysis.

We are going to use two types of soil for our analysis: dense clayey soil and sandy soil. Dense clay is chosen because of its high damping capacity, meaning it can absorb and dissipate a large portion of the energy from blast waves, making it a naturally effective protective layer for underground structures. Its cohesive nature also offers good stability under dynamic loading.

On the other hand, sandy soil is included in the analysis because desert regions, where sand is the predominant soil type, are common locations for military operations and forward operating bases. In such environments, bunkers must be constructed using the readily available material—sand. It is therefore critical to evaluate how a bunker performs when surrounded by sandy soil, which has lower damping properties compared to clay and may transmit more energy to the structure. By analyzing both, we simulate realistic field conditions and ensure the bunker design is robust across varying terrains and threat conditions.

In the FEM workbench of FreeCad, Under a new Analysis section, select the soil mound and a range of options would appear- select assign material to create material properties.

	Density (kg m ⁻³)	Young's Modulus (Pa)	Poisson Ratio
Clay soil	1800	40000000	0.4
Sand Soil	1600	25000000	0.3

Table 3.5 Material Properties of Clay and Sand, this will be required in the Assign Material option under the Analysis section of FEM workbench in FreeCAD. [\(10\)](#)

Once our materials are assigned, we have our bunker soil-mound compound ready as a realistic model.

3.6 MESHING

Meshing is a fundamental step in finite element analysis (FEA), where a complex geometry is divided into smaller, simpler elements, such as a smaller bar element, triangle, tetrahedra or hexahedra, that collectively approximate the shape and behavior of the original structure. These small elements are connected at nodes, and the governing equations of mechanics (such as stress-strain relationships) are solved at these nodes. This discretization allows the software to convert a continuous problem into a finite one that can be computed numerically. Without meshing, it would be nearly impossible to perform simulations on real-world geometries with varying thickness, curvature, and materials. The finer and more structured the mesh, the more accurate the results—though this also comes at the cost of increased computational effort. The purpose of meshing is to accurately capture how the structure behaves under loads, temperature changes, or other physical effects. Good mesh quality ensures that the load is distributed realistically and that stress concentrations, deformation patterns, and failure points can be reliably predicted. Mesh refinement, where elements are made smaller in regions of expected high stress or geometric complexity, helps achieve better precision without needing a uniformly fine mesh across the entire model. Therefore, meshing is not just a preparatory step but a critical process that directly affects the reliability and validity of the finite element results.

Now we are going to begin meshing our model. To make the process clearer and more manageable, we will first generate a mesh exclusively for the bunker. Refer to Fig 3.18 for that. This allows us to closely observe how the mesh adapts to the complex geometry of the structure, including the cavern unit, the access tunnel, and the varying thicknesses of the walls. Meshing the bunker separately also helps us fine-tune parameters like element size, shape, and refinement levels around areas of potential stress concentration.

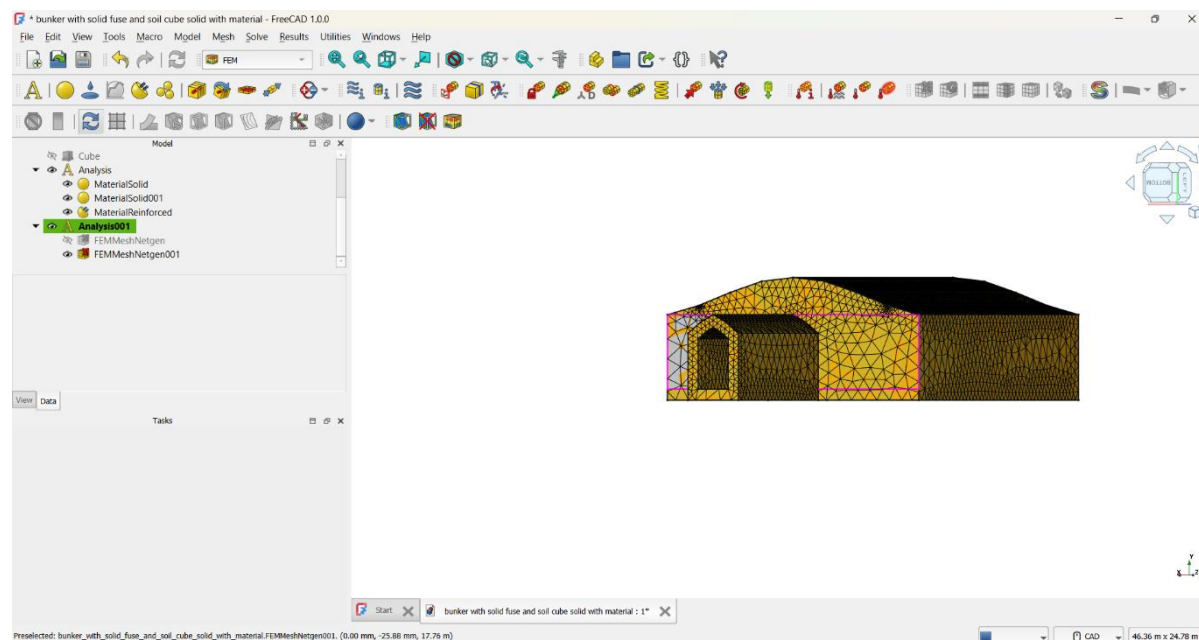


Fig 3.18 The mesh generated result of our blast resistant air raid shelter or bunker. Netgen was used to generate the meshing.

However, once this initial meshing is understood, our main goal will be to create a unified mesh that includes both the bunker and the surrounding soil mound. Meshing the soil and the bunker together as a single compound ensures that their interaction—especially in response to blast loading or ground movement—is accurately captured. The transition between materials (RCC and soil) must be well-resolved in the mesh to prevent unrealistic gaps or discontinuities. This combined meshing step is essential for reliable finite element analysis of the complete buried structure.

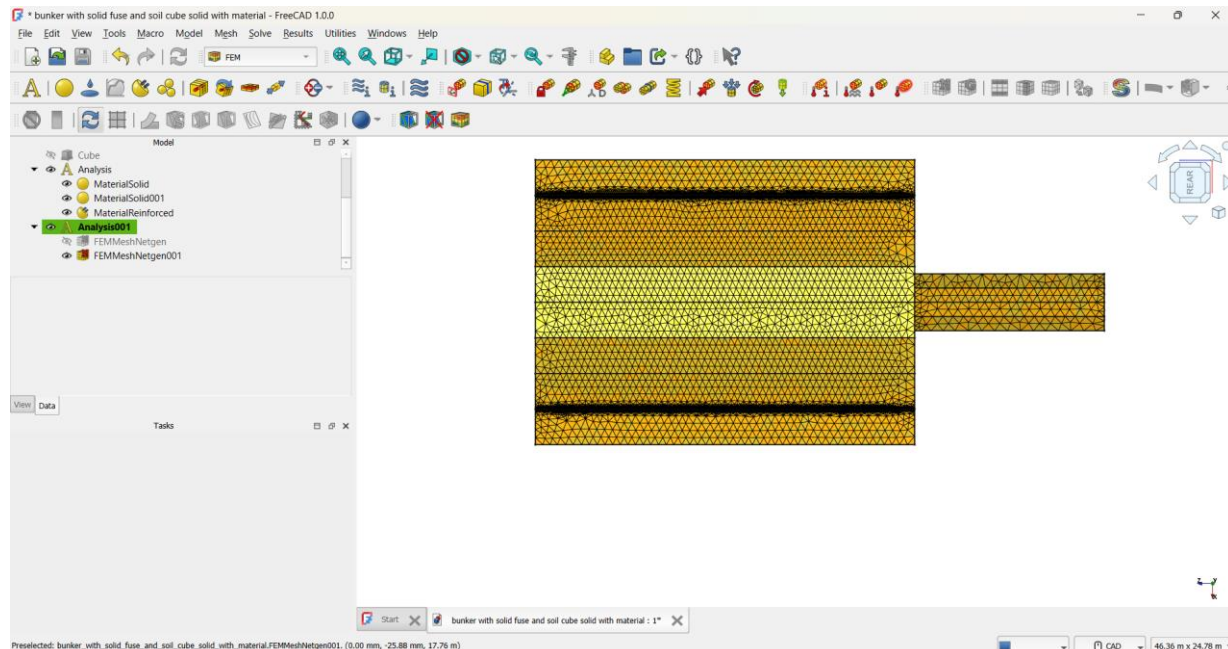


Fig 3.19 The top view of the bunker with the mesh. We can see finer meshing where it is suspected that behavior might not be subtle. Netgen meshing.

We will use the **FEM Workbench** in FreeCAD to carry out our meshing process. Within this workbench, we begin by creating a new analysis container that will hold all the simulation components, including materials, constraints, loads, and most importantly, the mesh. For generating the mesh, we will use **NetGen**, a built-in meshing tool in FreeCAD designed specifically for finite element methods.

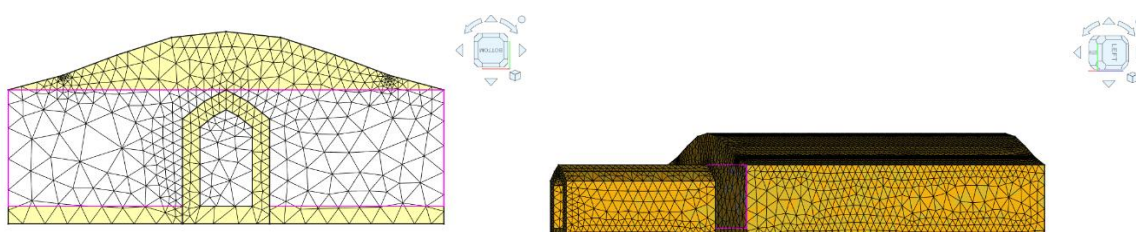


Fig 3.20 The front view of the meshed bunker. Tetrahedrons are generated to perform a 3D analysis of the volume

NetGen automatically creates a high-quality 3D mesh that conforms to the geometry of our model. This part of the process is entirely computational—the algorithm handles mesh generation without requiring manual input for every element. We simply select the solid to mesh, define basic parameters like maximum element size if needed, and let the software execute the meshing. Once the mesh is generated, it becomes the discretized version of our solid model, ready for the application of loads and boundary conditions in the finite element analysis.

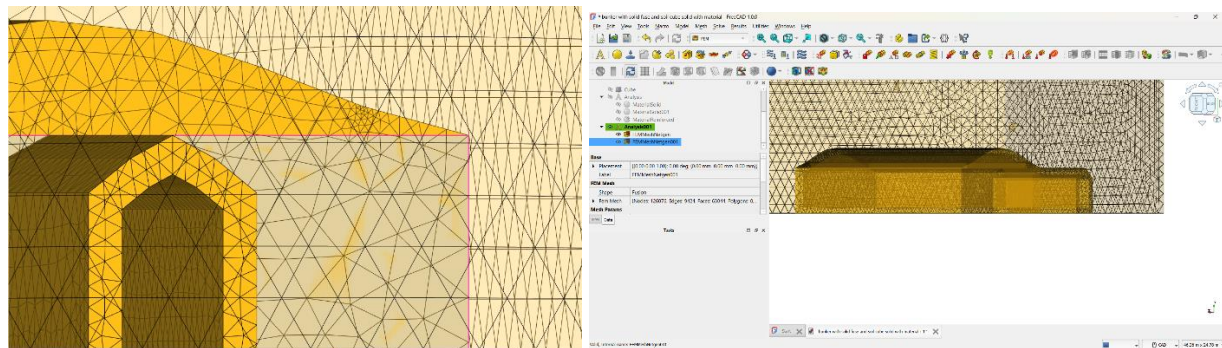


Fig 3.21 The meshed form of soil-bunker compound.

During the meshing process, a maximum element size of 1000 mm and a minimum size of 50 mm were selected to achieve a balanced resolution. This setup corresponds to **moderate** meshing, which was applied uniformly to both the soil mound and the bunker structure. The result was a well-distributed mesh that captures essential geometric and structural details without creating an excessive number of elements, ensuring both accuracy and computational efficiency for the upcoming finite element analysis. Thus, we get the following results:

Maximum	1000mm
Minimum	50mm
Nodes	420914
Triangles	18892
Tetrahedron	298585

Table 3.6 The results of the meshing of the soil cube

Maximum	1000mm
Minimum	50mm
Nodes	27335
Triangles	5268
Tetrahedron	16452

Table 3.7 The results of the meshing of the bunker fusion (fusion because it had been fused with Boolean)

3.7 BLAST LOAD

A blast load is a sudden, high-intensity pressure wave generated by an explosion. It acts over a very short duration and can cause significant structural damage due to its rapid rise in pressure, making it critical to consider in the design of protective structures like bunkers.

To accurately apply a blast load on a specific face or region of the model in an .inp file, it is crucial to identify the element ID or node ID corresponding to the target surface. Since the blast acts at a certain standoff distance, we must first locate the approximate coordinates on the model where the blast would impact.

For our case, the **standoff distance** is chosen as **20** meters, and based on the geometry of the soil mound, the blast point is located at the coordinates:

X = 8500 mm

Y = 1900 mm

Z = 40000 mm

From the mesh data exported in the .inp file, we search through the node list to find which node lies closest to these coordinates. The corresponding soil node ID at this position is found to be:

Node ID: 68037

This node, or more specifically, the element face connected to this node, will be used to define the blast surface in the input file. This ensures that the blast load is applied precisely at the intended location for realistic simulation results.

The formula used to estimate the peak overpressure from a blast —

$$P = 1772 \cdot \left(\frac{W^{1/3}}{R} \right)^{2.13} \quad \dots(3.9)$$

The Friedlander equation models the time history of overpressure from a blast wave at a given distance from an explosion. It is written as:

$$P(t) = P_s \left(1 - \frac{t}{t_d} \right) e^{-\alpha t/t_d} \quad \dots(3.10)$$

Where:

- P(t) is the overpressure at time ,

- P_s is the peak overpressure,
- t_d is the positive phase duration of the blast wave,
- α is a waveform shape parameter (typically ≈ 1.0 for TNT),
- $\left(1 - \frac{t}{t_d}\right) e^{-\alpha t/t_d}$: The term models the rapid rise and exponential decay of the pressure.

Approximation Used in Engineering

Engineers often don't simulate the full time history unless they're performing very advanced dynamic simulations. Instead, they use peak overpressure approximations — just the maximum blast pressure — to apply a static equivalent load for structural design.

This is where the empirical relation comes in:

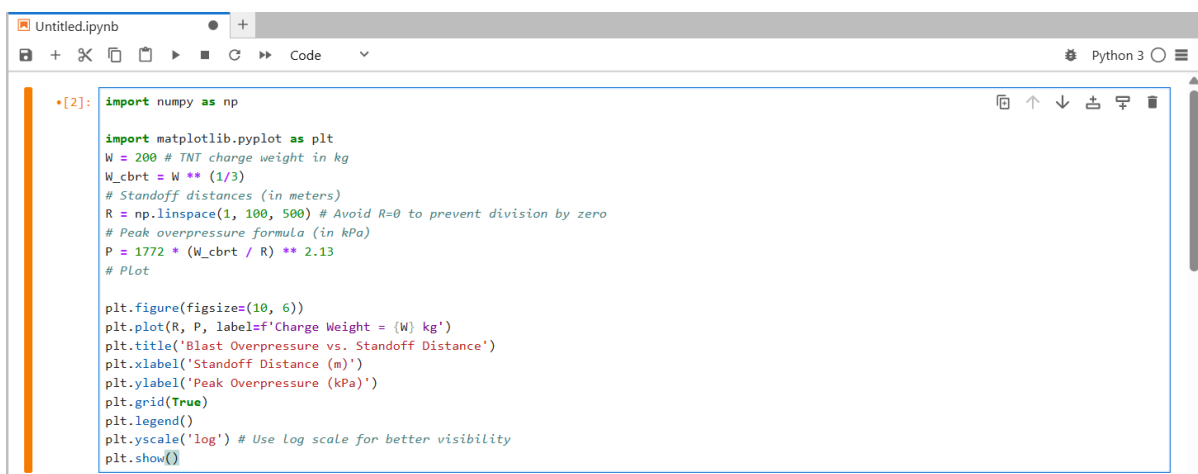
$$P = 1772 \cdot \left(\frac{W^{1/3}}{R}\right)^{2.13} \quad \dots(3.11)$$

This formula gives P in kilopascals (kPa)

- W = TNT equivalent charge weight (in kg)
- R = standoff distance (in meters)

It comes from curve fitting data generated by blast tests and approximates the peak pressure at a given distance for a given weight of TNT.

- The term reflects that the blast radius grows with the cube root of energy.
- The exponent 2.13 captures how quickly pressure decays with distance.
- The coefficient 1772 is a fitted constant valid for ideal air burst TNT detonations under standard atmospheric conditions.



```
[2]: import numpy as np
import matplotlib.pyplot as plt
W = 200 # TNT charge weight in kg
W_cbrt = W ** (1/3)
# Standoff distances (in meters)
R = np.linspace(1, 100, 500) # Avoid R=0 to prevent division by zero
# Peak overpressure formula (in kPa)
P = 1772 * (W_cbrt / R) ** 2.13
# Plot

plt.figure(figsize=(10, 6))
plt.plot(R, P, label=f'Charge Weight = ({W} kg')
plt.title('Blast Overpressure vs. Standoff Distance')
plt.xlabel('Standoff Distance (m)')
plt.ylabel('Peak Overpressure (kPa)')
plt.grid(True)
plt.legend()
plt.yscale('log') # Use log scale for better visibility
plt.show()
```

Fig 3.22 The Python snippet to show that our assumption for the Friedlander's time decay relation of the blast load is true.

Here is a simple python code to validate our assumption. Run this in the Python Console of Jupyter Notebook.

```
import numpy as np
import matplotlib.pyplot as plt
W = 200 # TNT charge weight in kg
W_cbrt = W ** (1/3)
# Standoff distances (in meters)
R = np.linspace(1, 100, 500) # Avoid R=0 to prevent division by zero
# Peak overpressure formula (in kPa)
P = 1772 * (W_cbrt / R) ** 2.13
# Plot
plt.figure(figsize=(10, 6))
plt.plot(R, P, label=f'Charge Weight = {W} kg')
plt.title('Blast Overpressure vs. Standoff Distance')
plt.xlabel('Standoff Distance (m)')
plt.ylabel('Peak Overpressure (kPa)')
plt.grid(True)
plt.legend()
plt.yscale('log') # Use log scale for better visibility
plt.show()
```

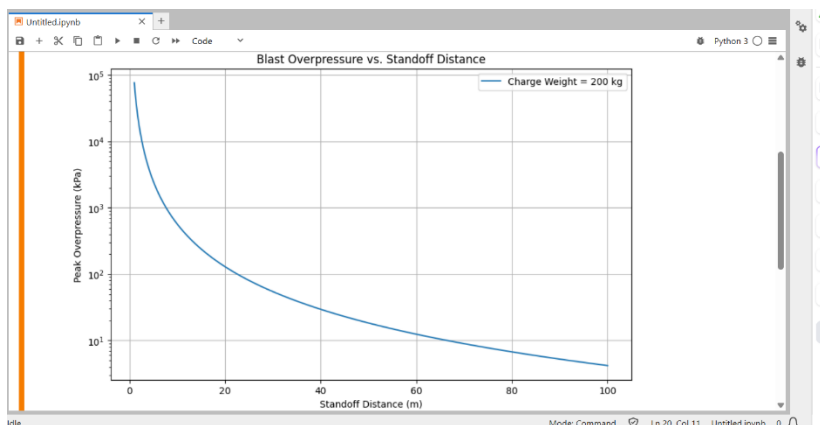


Fig 3.23 The Run Result (Shift+Enter) of the Python command for our assumption. It shows that it approximates the Friedlander's equation.

To apply a blast load, one must first determine the precise location on the model where the blast will have its maximum effect. This requires selecting an appropriate standoff distance and

translating that into spatial coordinates. For a standoff distance of 20 meters, and considering the dimensions and orientation of the soil mound, the approximate coordinate of interest is taken to be X = 8500 mm, Y = 1900 mm, and Z = 40000 mm. Within the .inp file, we search the node list to find the one closest to these coordinates; for this case, the relevant node was identified as node 68037. However, applying a pressure load directly requires an element face rather than a node, so we examine the element connectivity list to determine which element includes this node. Suppose we identify that element 8037 is the one containing it. This element then becomes the target for the blast load.

We are going to generate a plain text command and enter that into the .inp file on exporting our 3d mesh. The command is as follows:

```
*Amplitude, name=BlastAmp
0.0, 1.0,
0.001, 0.8,
0.003, 0.3,
0.005, 0.1,
0.008, 0.02,
0.010, 0.0

*Step, name=BlastStep, nlgeom=YES
*Dynamic, explicit
0.01, 1.0
*DLOAD, amplitude=BlastAmp
68037, P3, 0.1294
*End Step
```

We calculate the Pressure P Peak Amplitude from equation ... (3.11) for various chargeweight. On doing so, we get:

Charge-weight (kg) TNT Equivalent	Peak Over-pressure (P_s) Refer to eqn (3.11)
200	0.1294 MPa
500	0.2353 MPa

Table 3.8 The Over Pressure we will use in our plain text command for the corresponding chargeweight blast load

4. RESULTS AND DISCUSSIONS

Now that the .inp file has been prepared with the appropriate blast load input, the next step is to run the simulation using suitable finite element analysis software. Several platforms support .inp file formats, including Abaqus, CalculiX, ANSYS, Elmer FEM, Code_Aster, and SimScale. These solvers are capable of interpreting the mesh, boundary conditions, material properties, and the defined dynamic blast load, allowing us to observe the structural response of the bunker-soil system under high-intensity transient pressure. Among these, CalculiX is particularly accessible for academic use due to its open-source nature and compatibility with Abaqus syntax, while SimScale offers a cloud-based environment ideal for high-computation simulations without needing a powerful local machine.

After choosing the appropriate solver, we input the .inp file and set up the analysis type—typically an explicit dynamic analysis to accommodate the short-duration, high-pressure blast event. During the simulation, the software calculates stresses, displacements, and potential damage across the meshed structure over time. This step is crucial in assessing the survivability and design efficiency of the bunker under real-world explosive conditions. Post-processing tools within these platforms, or external ones like ParaView or SimScale, are then used to visualize and interpret the simulation output, helping in drawing meaningful conclusions about the behavior of the structure under blast loads.

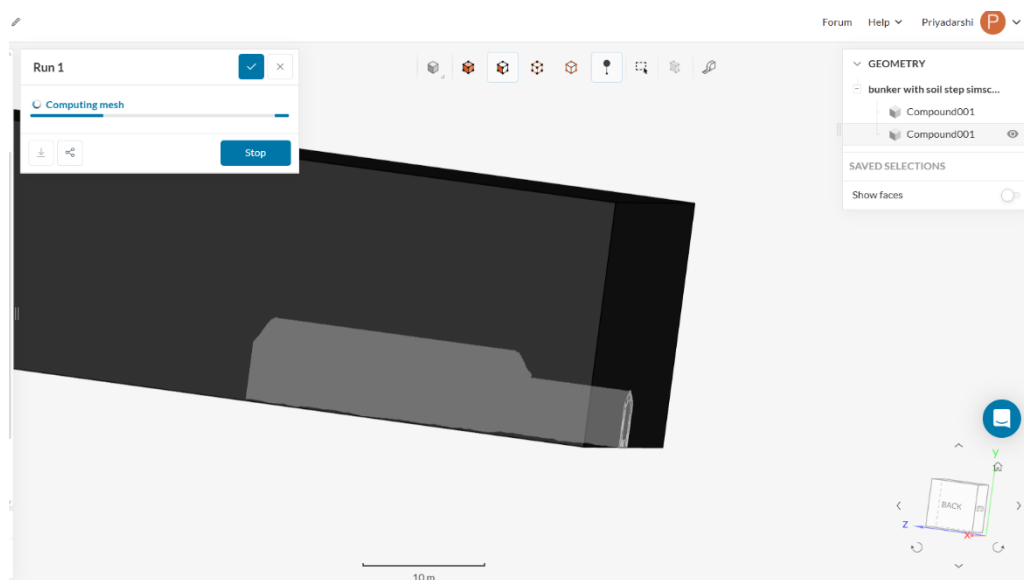


Fig 4.1 The uploaded mesh in SimScale, a quick FEM Simulator that runs on cloud based operation.

Simulation software interprets the meshed model—consisting of nodes and elements defined in the .inp file—and applies the material properties, boundary conditions, and loading scenarios (such as blast loads) to solve a system of equations based on finite element methods (FEM). Essentially, the software divides the entire structure into small, manageable pieces (elements),

and solves the governing physical equations (like Newton's laws for dynamics or Hooke's law for elasticity) at each node and element over time or under specific conditions. When a blast load is applied, the solver calculates how the pressure wave propagates through the soil and structure, how energy is absorbed, reflected, or transmitted, and how the bunker deforms, vibrates, or resists damage. These calculations are iterative and occur in very fine time steps, especially in dynamic simulations, enabling an accurate representation of how the structure responds under sudden and extreme loads.

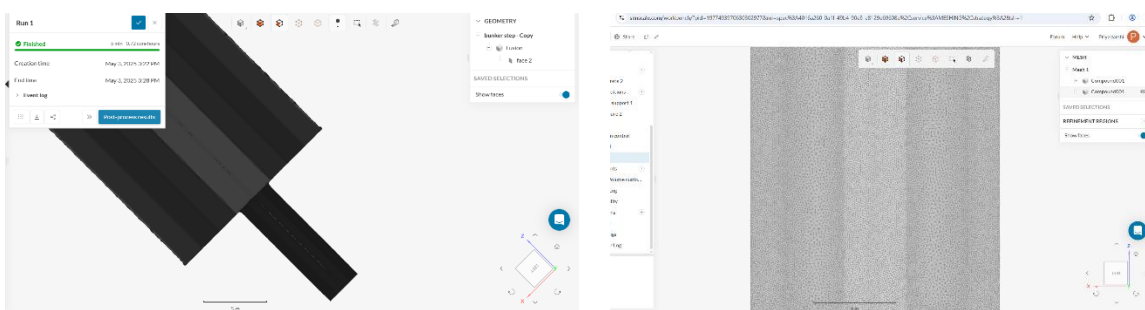


Fig 4.2 The Simulation that runs on SimScale. The second picture shows the dense tetragonal meshing.

For our purpose, we are going to use **SimScale** because it is fast, efficient, and operates entirely on the cloud, eliminating the need for heavy local computational resources. SimScale supports the import of .inp files and allows for setting up complex simulations like blast analysis through an intuitive web interface. After uploading our meshed model and defining the material properties, boundary conditions, and blast load as per our .inp setup, the simulation is initialized.

The simulation is then run on high-performance cloud servers, allowing for fast computation even for large-scale, nonlinear, or transient problems like blast loading. Within approximately two hours, the results are processed and made available for post-processing. These post-processed results include stress distribution, displacement fields, and energy absorption plots, helping us assess the performance and resilience of the bunker structure under explosive impact.

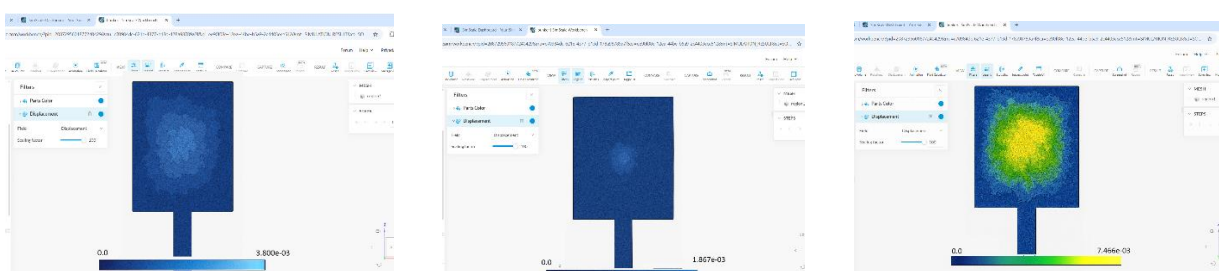


Fig 4.3 The Postprocessing results of the Bunker (Top View) under certain conditions, showing total deformation. First: 500kg charge weight blast at a standoff distance of 20m in Clay Soil, Second: 200kg charge weight blast at a standoff distance of 20m in Clay Soil, Third: 200kg charge weight at a standoff distance of 20 m in Sandy soil.

After the post-processing of our initial simulation, we proceed with a series of comparative simulations to study the effect of varying standoff distances, charge weights, and soil types on the structural behavior of the bunker. First, we simulate a 200 kg blast load at two different standoff distances—20 meters and 30 meters—in dense clayey soil. This allows us to observe how increasing the distance from the detonation point reduces the impact on the structure.

Next, we simulate both 200 kg and 500 kg blast loads at a 20-meter standoff distance in the same clay soil. This helps us evaluate how the magnitude of the explosive charge affects deformation and stress within the bunker-soil system. Finally, we perform a 200 kg blast simulation at a 20-meter standoff in sandy soil to assess how the soil type influences energy absorption and wave propagation. After obtaining all post-processed results, we compare the total deformation from each scenario to draw conclusions on the protective efficiency of different configurations and materials. This comparison guides us in optimizing bunker design for varying battlefield conditions.

We get the following results:

	20 m stand-off distance	30 m stand-off distance
Deformation when charge weight is 200kg	1.867×10^{-3} m	9.33×10^{-4} m

Table 4.1 Total Deformation when charge-weight is 200kg in Clay soil, at 20m and 30m standoff distance

	Total Deformation
200 kg Charge weight	1.867×10^{-3} m
500 kg charge weight	3.842×10^{-3} m

Table 4.2 Total Deformation when charge weight is 200kg and 500kg, both at clay and at 20m standoff

	Total Deformation For 200 kg blast at 20m
Clay soil	1.867×10^{-3} m
Sand Soil	7.466×10^{-3} m

Table 4.3 Total Deformation when charge weight is 200kg at 20m standoff, but in Clay soil and Sand soil

Thus, we observe clear trends in the deformation results under different conditions. For a 200 kg charge at a 20 m standoff distance in clayey soil, the total deformation is 1.867×10^{-3} m. When the standoff distance increases to 30 m, keeping the charge weight constant at 200 kg and the soil type unchanged, the deformation reduces significantly to 9.33×10^{-4} m. This demonstrates the exponential drop in structural response as the distance from the blast source increases.

Similarly, when we compare different charge weights at the same 20 m distance in clayey soil, the deformation increases from 1.867×10^{-3} m for 200 kg to 3.842×10^{-3} m for 500 kg, showing the effect of explosive magnitude. Lastly, when comparing the same 200 kg charge weight and 20 m standoff in different soils, we find that clay results in 1.867×10^{-3} m deformation, while sand leads to a much higher deformation of 7.466×10^{-3} m. This

highlights the weaker damping and lower confinement capacity of sandy soil in resisting blast impacts.

We make bar charts to have a visual comparison using Python:

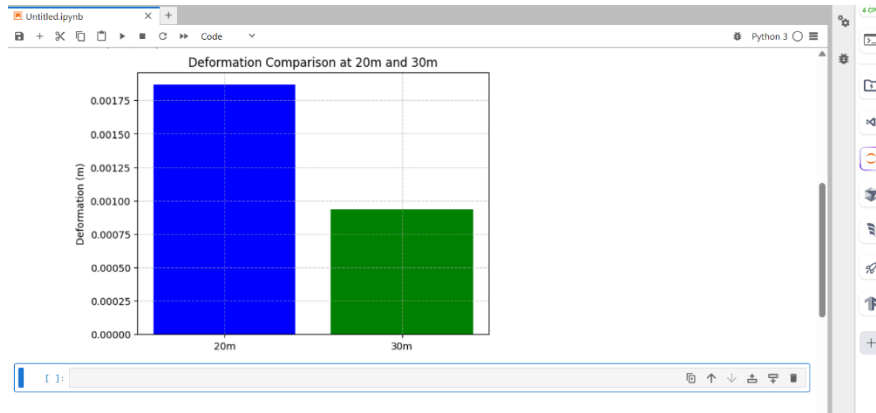


Fig 4.4 Comparison of total deformation at 20m and at 30m for both 200kg charge weight and at clay soil

```
import matplotlib.pyplot as plt

# Deformation values in meters
deformation_20m = 1.867e-3
deformation_30m = 9.33e-4

# Print comparison
print(f"Deformation at 20m: {deformation_20m} m")
print(f"Deformation at 30m: {deformation_30m} m")

# Ratio of deformation
ratio = deformation_20m / deformation_30m
print(f"\nRatio (20m / 30m): {ratio:.2f}")

# Plotting
labels = ['20m', '30m']
values = [deformation_20m, deformation_30m]
plt.bar(labels, values, color=['blue', 'green'])
plt.title('Deformation Comparison at 20m and 30m')
plt.ylabel('Deformation (m)')
plt.grid(True, linestyle='--', alpha=0.6)
plt.show()
```



Fig 4.5 Comparison of the total deformation incase of 200kg and 500kg charge weight, both at 20m and in clay soil

The above bar graph was generated using the following python code in Jupyter Notebook

```

import matplotlib.pyplot as plt

# Deformation values in meters
deformation_200kg = 1.867e-3
deformation_500kg = 3.842e-3

# Print comparison
print(f"Deformation for 200 kg: {deformation_200kg} m")
print(f"Deformation for 500 kg: {deformation_500kg} m")

# Ratio of deformation
ratio = deformation_500kg / deformation_200kg
print(f"\nRatio (500 kg / 200 kg): {ratio:.2f}")

# Plotting
labels = ['200 kg', '500 kg']
values = [deformation_200kg, deformation_500kg]
plt.bar(labels, values, color=['orange', 'red'])

plt.title('Deformation Comparison: 200 kg vs 500 kg (20m, Clay Soil)')
plt.ylabel('Deformation (m)')
plt.grid(True, linestyle='--', alpha=0.6)

plt.show()

```

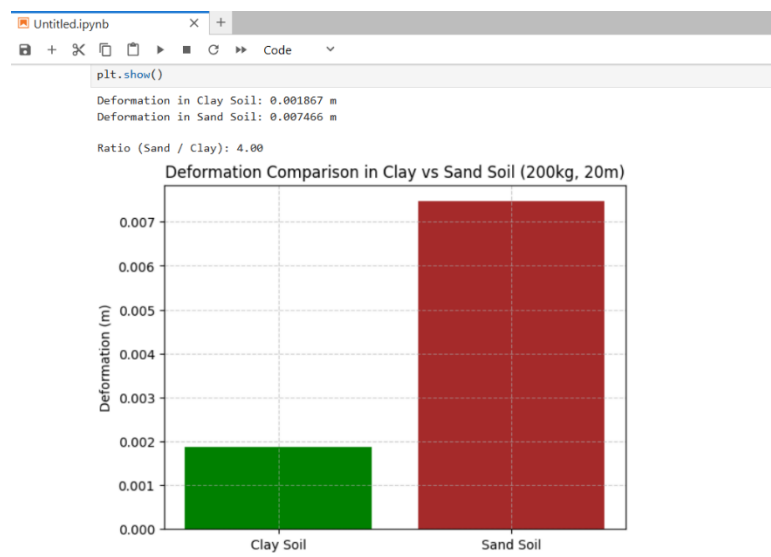


Fig 4.6 Comparison of the total deformation in case of clay soil and sand soil when the same blast load of 200kg is applied at 20m standoff distance.

```
import matplotlib.pyplot as plt

deformation_clay = 1.867e-3

deformation_sand = 7.466e-3

print(f"Deformation in Clay Soil: {deformation_clay} m")

print(f"Deformation in Sand Soil: {deformation_sand} m")

ratio = deformation_sand / deformation_clay

print(f"\nRatio (Sand / Clay): {ratio:.2f}")

labels = ['Clay Soil', 'Sand Soil']

values = [deformation_clay, deformation_sand]

plt.bar(labels, values, color=['green', 'brown'])

plt.title('Deformation Comparison in Clay vs Sand Soil (200kg, 20m)')

plt.ylabel('Deformation (m)')

plt.grid(True, linestyle='--', alpha=0.6)

plt.show()
```

When we compare the deformation results between clay and sand for the same blast load—200 kg of TNT at a 20-meter standoff distance—we observe a striking difference. In clay soil, the deformation is approximately 1.867 mm, whereas in sand soil, it rises to 7.466 mm. This means the deformation in sand is nearly four times greater than in clay. Such a difference highlights the significant role the type of soil plays in blast response.

Clay has a higher damping capacity, which enables it to absorb and dissipate a greater portion of the blast energy. This damping effect limits the amount of energy transmitted to the

structure, thereby reducing deformation. Sand, on the other hand, has much lower damping, allowing more of the blast energy to reach the structure and cause greater damage.

What's particularly important here is that when we compare other parameters—like increasing the blast load from 200 kg to 500 kg, or changing the standoff distance from 20 m to 30 m—the change in deformation is noticeable but not as dramatic as the one caused by switching from clay to sand. This shows that while both charge weight and distance affect the result, the nature of the soil medium has an even more dominant impact. The choice of soil can define the effectiveness of the structural response far more significantly than adjustments in other parameters.

Thus, when it comes to building a bunker, the choice of soil plays a critical role in determining its performance under blast loading. The soil mound acts as a natural damping medium, absorbing shock waves and reducing the energy transmitted to the structure. A well-chosen soil like clay, with better damping characteristics, can significantly limit deformation and enhance the bunker's protective capacity. The choice of soil is of paramount importance when one is constructing a blast resistant bunker because soil is the main compound that is going to absorb the shock wave and reduce the impact of the blast wave when it hits the structure underneath, that is our blast resistant bunker.

5. CONCLUSIONS

In conclusion, as the world witnesses an increase in wars and violent conflicts, the construction of bunkers has become more relevant and widespread. Countries like Israel have already integrated bunkers into everyday life, making them essential components of civilian safety. There are bunkers built in every locality, to even let passersby take shelter in times of need. In these times, bunkers serve not just as military structures but as shelters that protect human lives. Their design must be precise and well-informed — taking into account the grade of concrete, wall thickness, and reinforcement — but most crucially, the choice of soil. As shown in our study, soil plays a vital role in damping the vibrations from blast loads and, thus, reducing deformation in the structure. Without this damping effect, the very logic of burying a bunker underground would be undermined. Most modern bunkers have utilised this scope of engineering. The presence of soil as a protective layer is not just camouflage as the idea was back when very primitive bunkers were built in World War 1, it is structural. This topic also carries a deeply humanitarian relevance. I was particularly moved by the Ghibli film *Grave of the Fireflies*, where bunkers were shown to shelter civilians from US Air Raids, and also serve as a refuge of refugees to protect the last bit of human dignity.

6. CITATIONS

- (1) WIKIPEDIA (wikipedia.org) – Blast Wave, Bunker, Blast shelter, Air raid shelter...
- (2) IS 4991 (1968) Criteria for blast Resistant Design of Structures for explosion above ground
- (3) IS 5499 (1969) Code of Practice for construction of underground air-raid shelter
- (4) US Office Of Civilian Defense – Air Raid Shelter In Buildings
- (5) Research Gate (researchgate.org)
- (6) Nikos Pnevmaticos (Research Gate) researchgate.org
- (7) Materials Today Proceedings (B. Mahesh, P. Roy)
- (8) GP Nikishov (IIT Guahati)
- (9) IS 456 (2000)
- (10) Science Direct (sciencedirect.com) – Soil Modulus

7. BIBLIOGRAPHY

1. Dynamic Analysis of a military bunker subjected to blast load by M. Ashish Rajendra Yadav and Dr. S. K. Patil
2. Modification Modeling Of the Friedlander's Blast Wave Equation Using the 6th order of polynomial equation By H. K. Buwono, Najid
3. FEMA 453, Design Guidance for Shelters and safe rooms
4. A review on doomsday bunker by E. Ijmtst
5. Response of a vertical wall structure under blast loading by TP Nagyen, MT Tran
6. IS 4991 (1968) Criteria for blast Resistant Design of Structures for explosion above ground
7. Analysis of underground R.C.C. bunker subjected to blast load by Balsukuri Mahesh and Pronab Roy
8. Structural Design for Physical Security – American Society of Civil Engineers.
9. Dynamic Analysis of Military Bunkers Subjected to Air Blast- Mr. Ajmal Yusuf Shaikh, Prof. Sharif Shaikh
10. Dynamic Analysis Of Military Bunker subjected to Blast Load – Dipika Khandelwal, D.H. Tupe, G.R. Gandhe